MARTIN MARIETTA ENERGY SYSTEMS LIBRARIES
3 4456 0361178 6

CENTRAL RESEARCH LIBRARY
DOCUMENT COLLECTION

ORNL-2350
Physics and Mathematics

cy. 4

THE LID TANK SHIELDING FACILITY AT OAK RIDGE NATIONAL LABORATORY

PART II. DETERMINATION OF THE FISSION RATE OF THE SOURCE PLATE

D. R. Otis

CENTRAL RESEARCH LIBRARY
DOCUMENT COLLECTION
LIBRARY LOAN COPY
DO NOT TRANSFER TO ANOTHER PERSON
If you wish someone else to see this document, send in name with document and the library will arrange a loan.

OAK RIDGE NATIONAL LABORATORY
operated by
UNION CARBIDE CORPORATION
for the
U.S. ATOMIC ENERGY COMMISSION

Erratum to Internal Distribution of ORNL-2350:

On page 9, line 13, change to read:

yielded a value of 0.575 ± 5% for the fractional absorption factor. This

Printed in USA. Price $1.50. Available from the
Office of Technical Services
Department of Commerce
Washington 25, D.C.

LEGAL NOTICE

This report was prepared as an account of Government sponsored work. Neither the United States, nor the Commission, nor any person acting on behalf of the Commission:

A. Makes any warranty or representation, expressed or implied, with respect to the accuracy, completeness, or usefulness of the information contained in this report, or that the use of any information, apparatus, method, or process disclosed in this report may not infringe privately owned rights; or

B. Assumes any liabilities with respect to the use of, or for damages resulting from the use of any information, apparatus, method, or process disclosed in this report.

As used in the above, "person acting on behalf of the Commission" includes any employee or contractor of the Commission, or employee of such contractor, to the extent that such employee or contractor of the Commission, or employee of such contractor prepares, disseminates, or provides access to, any information pursuant to his employment or contract with the Commission, or his employment with such contractor.

UNCLASSIFIED

ORNL-2350

Copy No. 4

Contract No. W-7405-eng-26

Neutron Physics Division

THE LID TANK SHIELDING FACILITY AT OAK RIDGE NATIONAL LABORATORY
Part II. DETERMINATION OF THE FISSION RATE OF THE SOURCE PLATE*

D. R. Otis**

Date Issued

JUL 7 1959

OAK RIDGE NATIONAL LABORATORY
Oak Ridge, Tennessee
operated by
UNION CARBIDE CORPORATION
for the
U. S. ATOMIC ENERGY COMMISSION

*Other reports in this series are ORNL-2531 (Part I) and ORNL-2587 (Part III). The information in this report was summarized in ORNL-2081, p. 163 (1956).

**On assignment from Convair, San Diego.

UNCLASSIFIED

MARTIN MARIETTA ENERGY SYSTEMS LIBRARIES

3 4456 0361178 6

ABSTRACT

Following the installation of the second Lid Tank Shielding Facility source plate, a thin uranium disk identified as SP-2, a series of experiments were performed to determine its fission rate. Three independent methods were used, one based on the rate of absorption of the thermal neutrons incident on the plate, another based on the rate of fast-neutron production within the plate, and a third one based on the power dissipation within the plate. Discussions of the methods, all of which yielded consistent results, are presented, along with a description of the source plate. A weighted average of the fission rates determined by the three methods gave a result of 1.66×10^{11} fissions/sec $\pm$ 5% for the standard incident thermal-neutron flux. With an assumed energy dissipation of 200 Mev/fission, a typical reactor having this fission rate would release 5.22 watts of heat power. The calibration of the SP-2 allowed a re-evaluation of the power of the first LTSF source plate, the SP-1. The revised "effective" neutron power for SP-1 is 1.7 watts $\pm$ 11%.

TABLE OF CONTENTS

		Page No.
	ABSTRACT	ii
	AUTHOR'S PREFACE AND ACKNOWLEDGEMENTS, EDITOR'S NOTE	iv
	INTRODUCTION	1
I.	DESCRIPTION OF THE LTSF SOURCE PLATE (SP-2)	3
II.	DETERMINATION OF THE SOURCE STRENGTH OF THE SP-2	7
	Method 1: Fission Rate Determination by Estimation of Incident Thermal-Neutron Absorption Rate in the Source Plate	8
	Calculation of the Fractional Absorption Factor	8
	Determination of Incident True Thermal-Neutron Flux	12
	Calculation of the Fission Rate	13
	Method 2: Fission Rate Determination by Estimation of Neutron Production Rate in the Source Plate	16
	Method 3: Fission Rate Determination by Estimation of Power Dissipation in the Source Plate	21
	Summary of Methods 1, 2, and 3 in Terms of Power	27
III.	RE-EVALUATION OF THE POWER OF THE FIRST LTSF SOURCE PLATE (SP-1)	28
App. A.	FISSION ENERGY ABSORBED BY THE SP-2	31
App. B.	ESTIMATED POWER OF SP-2 VERSUS HEATING TIME	38
App. C.	DETERMINATION OF SOURCE PLATE LEAKAGE FACTORS	43
App. D.	LIST OF FIGURES	45

AUTHOR'S PREFACE AND ACKNOWLEDGEMENTS

The calibration of the new LTSF source plate, though seemingly a simple task, required the expenditure of approximately four man-years. A six-months period beginning in October, 1955, was spent in gathering the necessary experimental data and another six-months period was spent in analyzing the data. The experimental work was performed by W. J. McCool* and J. M. Miller with the assistance of a staff of technicians which included J. R. Taylor, E. B. Beckham, D. R. Hendrix, B. M. Millican, and H. J. Jarvis. Most of the members of the technical staff of the LTSF contributed to the analysis of the data in one way or another, and where a staff member has given a specific contribution he is acknowledged in the text. As supervisor of the LTSF, R. W. Peelle guided the design and execution of the calibration experiments and contributed to the interpretation of the data and the preparation of the final report. As earlier leaders of the group, C. L. Storrs and G. T. Chapman had important influences on the initiation of the work and the procurement of the enriched uranium and other necessary hardware. The ORNL Metallurgy Division and the Instrumentation and Controls Division aided in the design and fabrication of many of the components. Of the four man-years required for this work, the author contributed eight man-months, all of which were directed toward analysis of the data and preparation of the report.

*On assignment from Pratt and Whitney Aircraft.

EDITOR'S NOTE

The author's participation in this work was carried out while he was on assignment to the Laboratory from Convair, San Diego. He was recalled in February, 1957, at which time this report was in reasonably complete form. In the process of final editing a few corrections have been made; however, corrections which would have resulted in a change that would be a small fraction of the quoted error were not included in the final result.

INTRODUCTION

The Lid Tank Shielding Facility[1] (LTSF) was the first facility constructed at the Oak Ridge National Laboratory for the purpose of testing radiation shields. Completed in 1949, it consists basically of a large water-filled steel tank (called the Lid Tank) which has a disk-shaped fission source mounted in one wall. The tank is mounted like a "lid" over the outer end of a horizontal hole through the concrete shield of the ORNL Graphite Reactor so that the source, a circular plate of uranium mounted in the inner tank wall, is exposed to thermal neutrons from the reactor. In a sense the uranium source plate "converts" the thermal neutrons from the hole (called the "Core Hole") into a fission spectrum, and because of this it is sometimes referred to as a "converter plate."

When the LTSF was first constructed, the source plate assembly consisted of rows of natural uranium slugs stacked one upon the other and held between layers of masonite as shown in Fig. 1. This source plate, since designated as SP-1, suffered from several limitations: (1) its power was quite low and not accurately known, (2) its geometry was far from the ideal thin disk shape, and (3) the self-absorption of gamma rays and neutrons could not be accurately calculated. Some of these limitations were recognized even in 1949, but much greater uncertainties in shield design needed to be resolved quickly. In recent years, however, it has been necessary and plausible to design shields more closely to given tolerance limits, and this has required a more careful approach to the problem. Before LTSF data could be used to satisfy such requirements, the radiation source had to be described in greater detail. Since this was impossible with the original source plate, it became apparent that a new source plate was necessary.

---

1. The Lid Tank Shielding Facility at Oak Ridge National Laboratory, Part I. Description, ORNL-2531 (to be published).

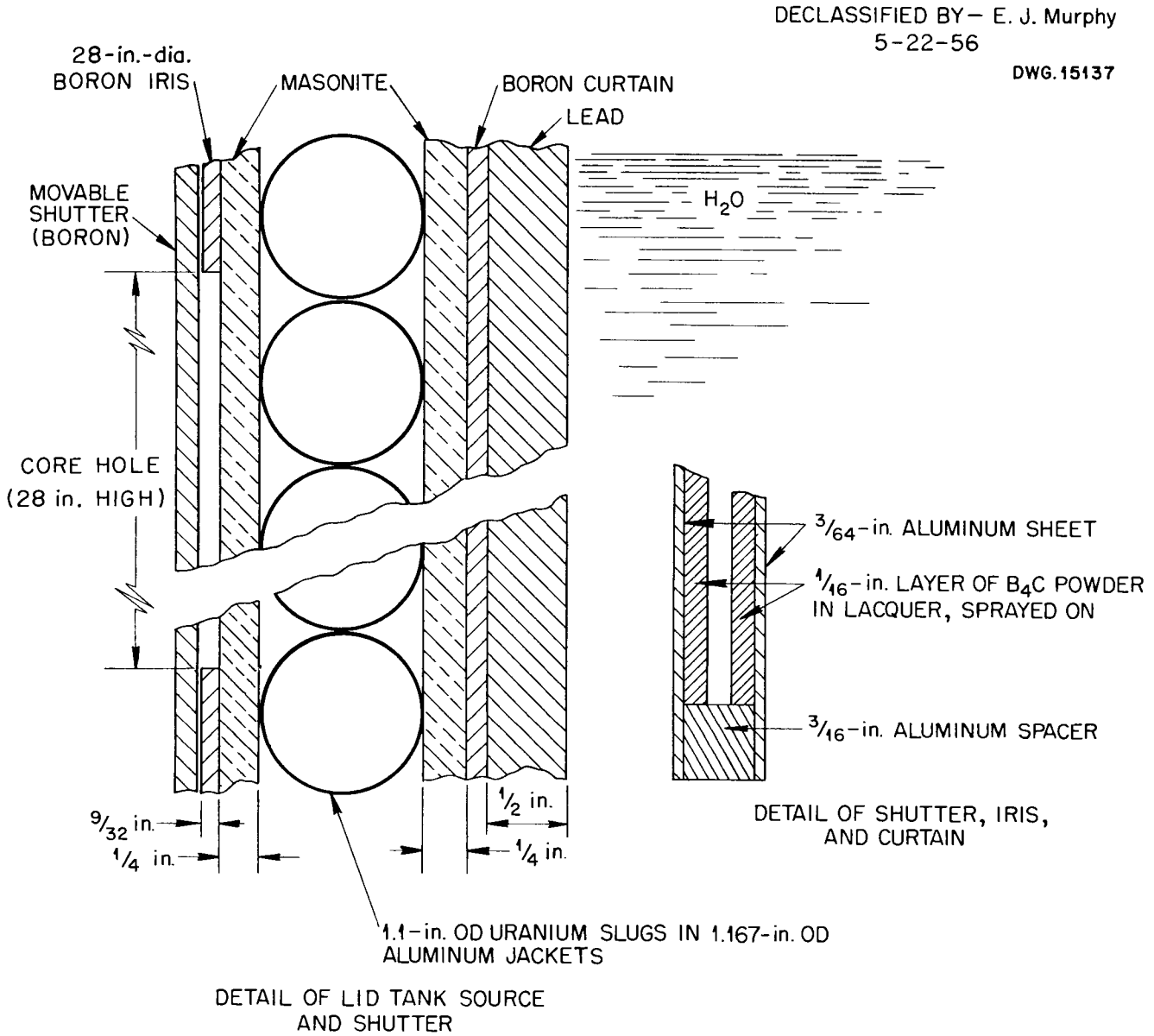

Fig. 1. Sectional View of the First LTSF Source and Shutter (SP-1).

Consequently, a second source plate assembly was designed in which the three restrictions listed above are largely overcome. This source plate, designated as SP-2, replaced SP-1 in October, 1955. It is the purpose of this report, which is Part II of a series of three reports on the LTSF,[1,2] to describe the new source plate and to report the experiments performed to determine its power. A better estimate of the "effective" power of the old source plate, which was made possible by a comparison of the experimental data obtained with the two source plates under similar conditions, is also presented. The numerical values obtained in this work were reported previously,[3] but a complete description was not given.

I. DESCRIPTION OF THE LTSF SOURCE PLATE (SP-2)

The new source plate is a thin circular disk of uranium 28.0 in. in diameter. It consists of 20.8% U^{235} and 79.2% U^{238} and was fabricated as two half-disks by rolling uranium ingots of this composition and then machining them to size. The average thicknesses of the upper and lower half-disks are 0.0617 and 0.0576 in., respectively; the nominal thickness is quoted as 0.060 in. The line of division is from the upper right to the lower left, if the observer is facing the Graphite Reactor.

The source plate assembly is composed of several regions illustrated in Figs. 2 and 3. The uranium disk is supported by an aluminum framework which also supports a 1/8-in.-thick boral plate on the Lid Tank side of the disk and a 1/8-in.-thick heater plate on the reactor side. The boral prevents diffusion of thermal neutrons from the Lid Tank back into the source plate,

---

2. The Lid Tank Shielding Facility at Oak Ridge National Laboratory, Part III. Instrumentation, ORNL-2587 (to be published).
3. D. R. Otis, Applied Nuc. Phys. Ann. Prog. Rep. Sept. 10, 1956, ORNL-2081, p. 163.

UNCLASSIFIED
ORNL-LR-DWG 13591A

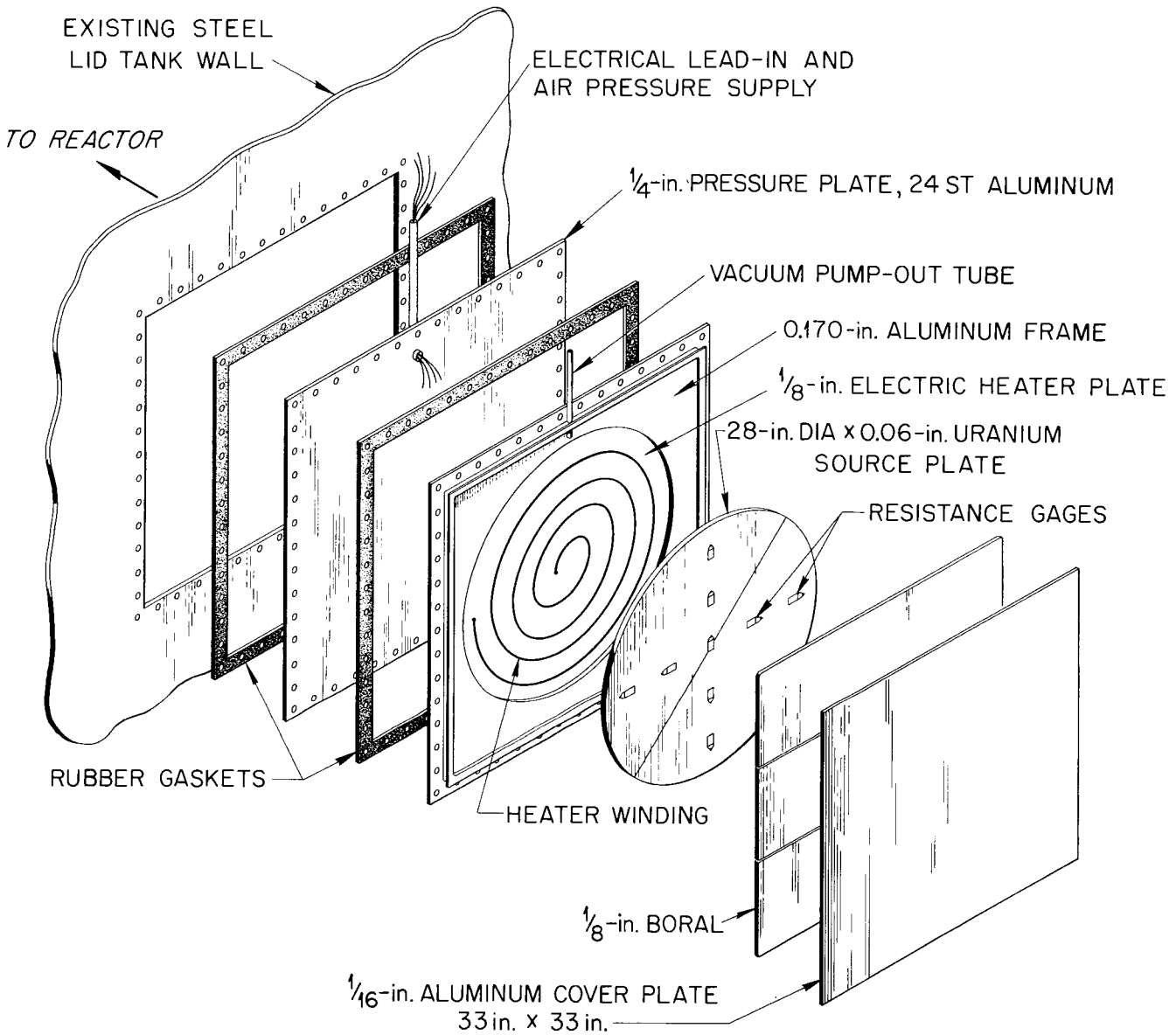

Fig. 2. Exploded View of the Second LTSF Source Plate Assembly (SP-2)

UNCLASSIFIED
2-01-057-0-438

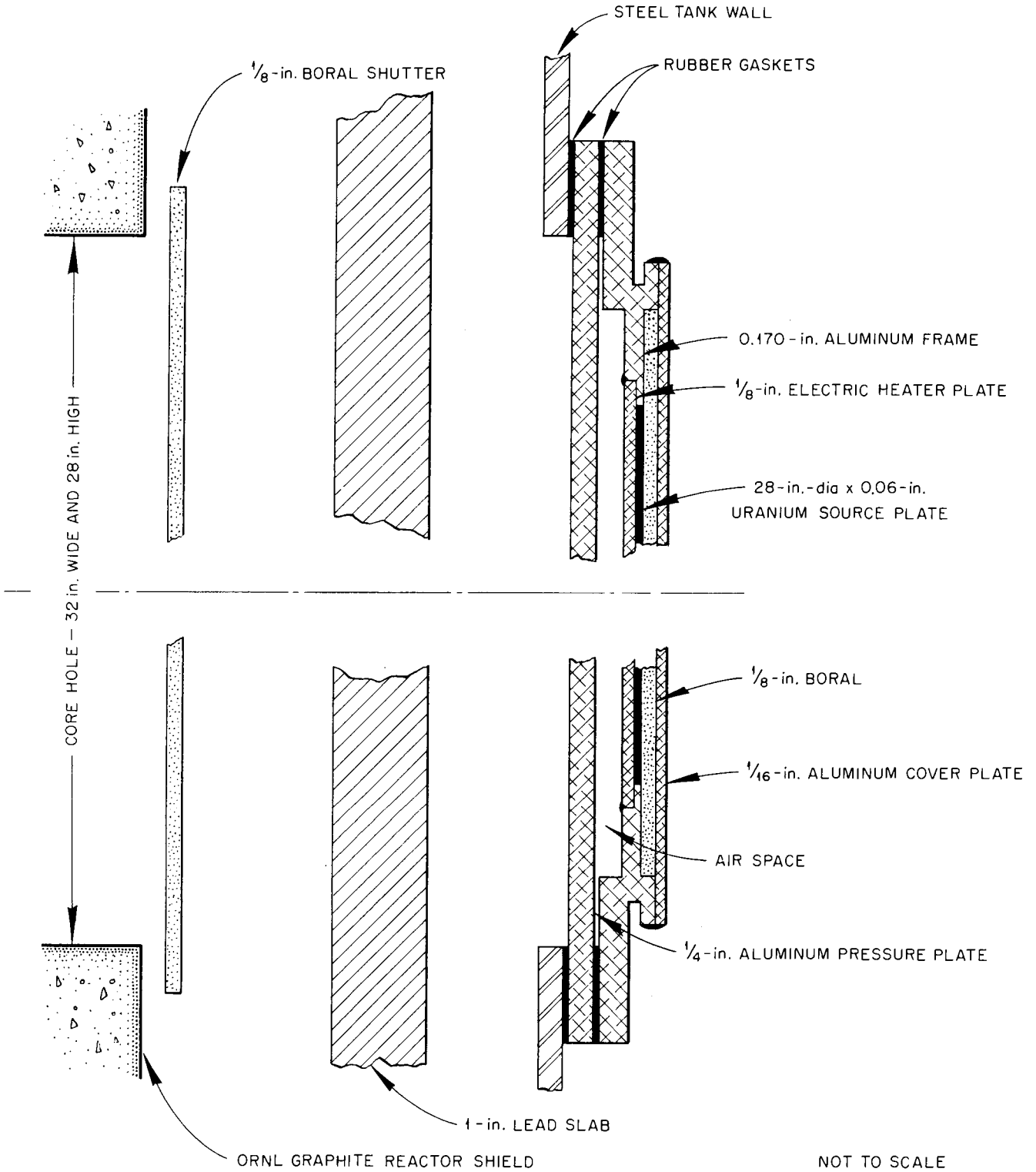

Fig. 3. Sectional View of the Second LTSF Source Plate (SP-2) Showing Its Position Relative to the Boral Shutter and the ORNL Graphite Reactor.

which process would make the power of the source plate somewhat dependent upon the composition of shields placed in the Lid Tank. The heater plate is included in the assembly so that the uranium disk can be electrically heated with any known power. The heating is accomplished with a No. 30 Formvar-insulated copper wire cemented into a spiral groove machined in the heater plate with a pitch of 1/2 in. This provides a relatively uniform electrical power distribution over the source plate.

The temperature of the source plate can be measured with resistance gages cemented to the uranium at nine locations on the side adjacent to the boral sheet. The gages are Baldwin-Lima-Hamilton Corporation type T-14 gages, having a response of approximately 0.5 ohm/$^{\circ}$F and a total resistance of 200 ohms.

On the reactor side of the heater plate there is 1/4-in.-thick aluminum pressure plate which carries the hydrostatic pressure load imposed upon the assembly by the liquid in the Lid Tank. The air space between the heater plate and the pressure plate is slightly pressurized (by about 1.4 psig) to prevent the heater plate and the source plate from being distorted under the hydrostatic pressure and to keep water from entering this region. The air pressure is supplied through the lead-in pipe that carries the electrical wires to the source plate resistance gages and the heater.

An aluminum cover plate is welded over the outside of the aluminum frame supporting the uranium disk, boral plate, and heater. A small mechanical vacuum pump removes gas from the region between the heater plate and cover plate, allowing hydrostatic pressure to force the uranium into contact with the spiral electric heater. The outlet of the vacuum pump exhausts into the cooling air outlet of the ORNL Graphite Reactor to prevent air contamination from any gaseous fission products.

The entire source plate assembly is mounted over a square hole in the Lid Tank wall in the direct path of thermal neutrons coming from the Core Hole.

A 1/8-in.-thick boral shutter,* shown in Fig. 3, is used to intercept and absorb thermal neutrons from the reactor to enable background measurements. A 1-in.-thick lead slab between the boral shutter and the source plate assembly is used to reduce background within the Lid Tank from gamma rays originating in the Graphite Reactor.

The source plate assembly described above represents a considerable improvement over the original assembly. First of all, the power of the new source plate is about three times higher than that of the first one. (Any further increase in power would require additional shielding around the Lid Tank for the protection of personnel.) The greatest improvement is in the geometry; that is, the thin uranium disk approaches the ideal, although this is partially compromised by the lack of uniform distribution of incident thermal neutrons. This approach to the ideal allows certain transformations that are used in the interpretation of the LTSF data to be applied with greater confidence and more accurate estimates of the self absorption of gamma rays and neutrons to be made.

II. DETERMINATION OF THE SOURCE STRENGTH OF THE SP-2

The new source plate was designed so that its power could be measured. Experiments since its installation have made it possible to estimate its strength by three independent methods, each dealing with a different property of the fission reaction: the first with the rate of absorption of neutrons in the source plate, the second with the rate of neutron production in the source plate, and the third with the power dissipation within the source plate. In the pages which follow, each of these methods and the corresponding source strength estimates are discussed.

In following through the description of the experiments some confusion could arise in connection with the word "normalize" since it is used in two

*Note added in 1959: The thickness of this boral shutter is now 1/4 in., but since the increase in the thickness has only a small effect on the quoted power no attempt was made to correct for it in this report.

different senses. The first usage applies to the normalization of all LTSF data to a constant power. This means that the data are corrected to a standard thermal-neutron flux in the Core Hole. This flux varies with the power and fuel loading of the reactor, and it is normally monitored with a boron-lined ionization chamber located within the hole. The second use of the word "normalize" is in relation to the experiments themselves. The 1-in.-thick lead gamma-ray shield shown in Fig. 3 was installed after some of the calibration experiments had been performed. Since this slab affects the power of the plate, all the experiments were normalized to this standard arrangement.

Method 1: Fission Rate Determination by Estimation of Incident Thermal-Neutron Absorption Rate in the Source Plate*

One method for determining the source strength of the SP-2 consisted in a determination of the absorption rate of thermal neutrons incident on the source plate. As a first step the fraction of the incident thermal neutrons that are absorbed in the source plate (called the "fractional absorption factor") was calculated using foil experiments as a guide. In the second step the incident thermal-neutron flux was measured. Finally, these results were combined with known nuclear parameters, the source plate area, and geometric corrections to obtain the source strength in terms of fissions per second.**

Calculation of Fractional Absorption Factor. The fractional absorption factor was determined by calculating the transmission through the uranium source

---

*This method was developed by and the experiments were performed by W. J. McCool and J. M. Miller. The analysis was performed by W. R. Burrus. This section of the report was also prepared by Burrus.

**Note added in 1959: In this calculation the fissions caused by fast neutrons originating in the uranium source plate itself have been ignored. L. Dresner (see Ref. 4) in a rather precise procedure, estimated that the effect of first-generation neutrons would necessitate a correction of 1.84% and that the effect of succeeding generations would increase the total correction to 1.94%. This correction is not considered in this report since it is much smaller than the estimated error. Prior to the Dresner study, a first-generation effect was calculated as part of this source plate power study on the basis of eye-averaged fast-neutron cross sections and a reduction of Eq. A-2 in Appendix A; the result indicated an effect of 1.7%.

4. L. Dresner, Estimate of the Fast Effect in the Lid Tank Source Plate, ORNL-CF-59-3-67 (1959).

plate for thermal neutrons having estimated energy and angular distributions. It was assumed that the energy spectrum could be represented by a Maxwell-Boltzmann distribution for which the effective temperature of the neutrons was estimated from the temperature of the graphite reflector of the ORNL Graphite Reactor. The temperature of the neutrons leaving the graphite is lower than the temperature of the graphite itself owing to variations in the diffusion parameters with energy.[5] For an approximate graphite temperature of 370°K, an effective temperature of 280°K was estimated for the thermal neutrons incident on the source plate. Since these neutrons are fairly well collimated through the Core Hole they can be considered to be normally incident on the source plate, ignoring a possible scattered component from the walls of the Core Hole and neighboring materials. These assumptions yielded a value of 0.575 ± 5% for the * Fractional absorption ~~thermal utilization~~ factor. This value was used in the final calculation.

Because of the uncertainties involved in choosing the effective temperature and the angular distribution for this calculation, an experiment was performed to check the internal consistency of the assumed values. Gold foils were placed on each side of slabs of source plate material sandwiched between aluminum sheets as shown in Fig. 4a, and the assembly was exposed to the thermal-neutron flux of the Core Hole in the position shown in Fig. 5. The results of the foil activation measurements as a function of uranium thickness (62 to 187 mils) were consistent with the 280°K effective neutron temperature and perpendicular incidence assumed above.

In order to obtain some idea of the over-all error involved in the assumption of particular angular and energy distributions for the incident

---

5. F. L. Tolstov, F. L. Shapiro, and I. V. Shtranikh, Average Neutron Velocities in Various Media, reported at the July, 1955 session of the Acad. Sci. USSR.

* See erratum

UNCLASSIFIED
2-01-057-0-439

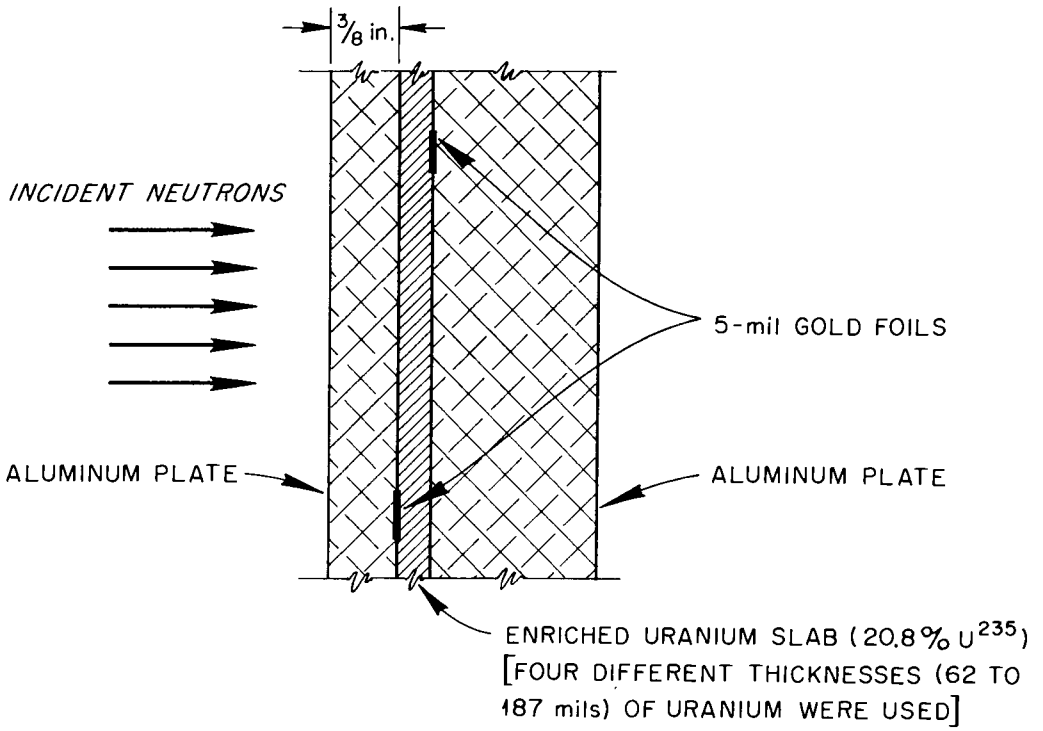

Fig. 4a. Mockup for Thermal Utilization Experiment.

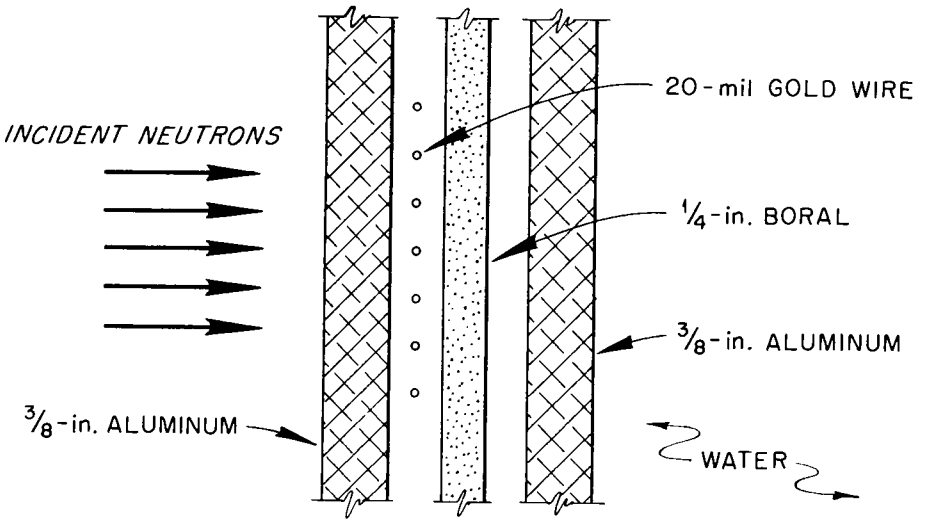

Fig. 4b. Gold Wire Mockup for Flux Determination.

UNCLASSIFIED
2-01-057-0-440

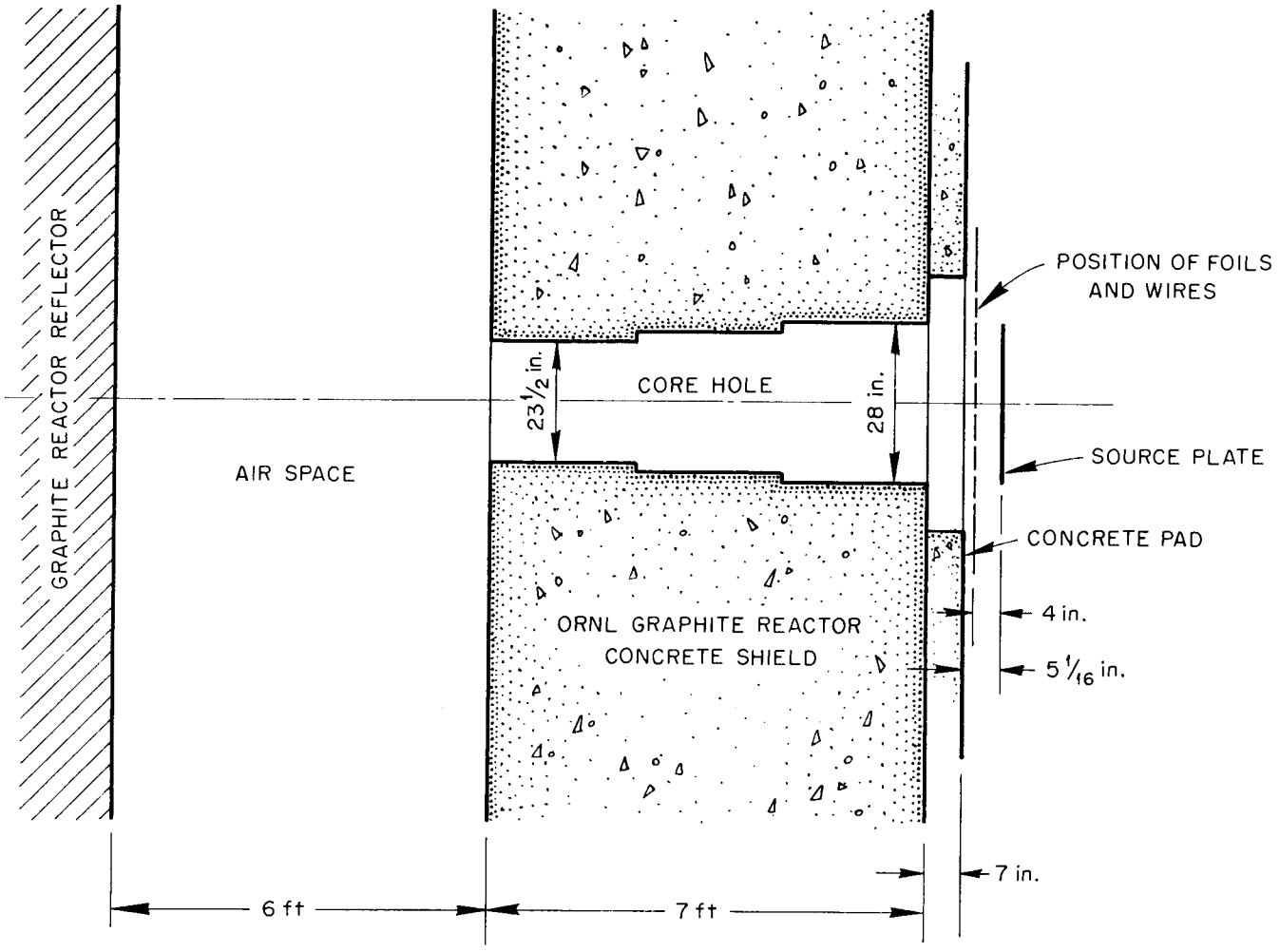

Fig. 5. Vertical Cross Section of the ORNL Graphite Reactor Core Hole Showing the Position of the Gold Foils and Wires in the Thermal Utilization Experiment. (Lid Tank not shown)

neutrons, an effective neutron temperature $40^{\circ}K$ higher ($320^{\circ}K$) was chosen as the highest plausible value. The angular distribution was postulated to be some combination of perpendicular and $\cos\theta$ components, where θ is the angle between the neutron direction and the perpendicular to the source surface. A nonperpendicular component could arise from scattering effects, and the $\cos\theta$ term is supposed to represent such an effect. In order to fit the foil activation data it was necessary to choose a combination of 70% perpendicular and 30% $\cos\theta$. Using this combination of temperature and angular distribution did not appreciably change the fractional absorption factor, but the final power estimate was changed by about 8% because the temperature and angular distribution also affect the calculation of the neutron current incident upon the plate based on the neutron density measurements described below. The error estimate of 5% given for the fractional absorption factor was based upon this over-all difference generated by assuming a different effective temperature.

Determination of Incident True Thermal-Neutron Flux. The true thermal-neutron flux incident on the SP-2 was determined from the activation of a set of 20-mil-dia gold wires which were exposed between the source plate and the reactor at the position shown in Figs. 4b and 5. As a check on the wire exposures, a few 1-cm-square by 5-mil-thick gold foils were also exposed at this position. During such exposures a boral sheet was inserted between the wires and foils and the Lid Tank to prevent the detection of thermal neutrons from the direction of the LTSF.

The foils were counted with a well-type scintillation counter* which was calibrated against a standard high-pressure ionization chamber* and was cross-checked with standard gold solutions obtained from the National Bureau of Standards. The wires were counted on a collimated scintillation wire scanner which had been calibrated against the well counter. In the calculation of the fluxes from the gold activations, the value of the gold

*This equipment was borrowed from the ORNL Isotopes Division.

2200 $m \cdot sec^{-1}$ cross section used was 98.7 barns (Ref. 6). The data were corrected for self protection, the assumed temperature distribution of the neutrons, and epithermal activation via the 4.9-ev gold resonance.

The fluxes calculated on the basis of the foil data agreed with those calculated on the basis of the wire data within 3%. This slight difference could have been caused by a shift in the reactor power, although, as explained earlier in this report, such shifts are ordinarily compensated for by monitoring the flux in the Core Hole and normalizing all the data to a standard value. In this case, however, the monitor was probably affected by the foils and wire mockup assemblies. The possibility that the error was introduced in the correction factors also exists.

An isoflux plot based on the uncorrected wire measurement is shown in Fig. 6. An average true thermal-neutron flux of 1.35×10^8 neutrons$\cdot cm^{-2} \cdot sec^{-1} \pm 4.6\%$ was obtained by graphical integration from these data. Since this value is for a position closer to the reactor than the source plate itself, it was necessary to introduce a geometrical correction based on the inverse square law in the calculation of the fission rate described below.

Calculations of the Fission Rate. The strength P of the source plate in terms of fissions per second was calculated from the following equation:

$$P = \phi f v G N L B S, \tag{1}$$

where

ϕ = average incident true thermal-neutron flux (assumed to be perpendicular to the surface of plate),

f = fractional absorption factor,

v = fraction of neutrons absorbed that result in fission (reported in App. A),

---

6. This is consistent with the value (98.9 ± 3) barns quoted in Neutron Cross Sections, by D. J. Hughes and R. B. Schwartz, BNL-325, Second Edition (1958).

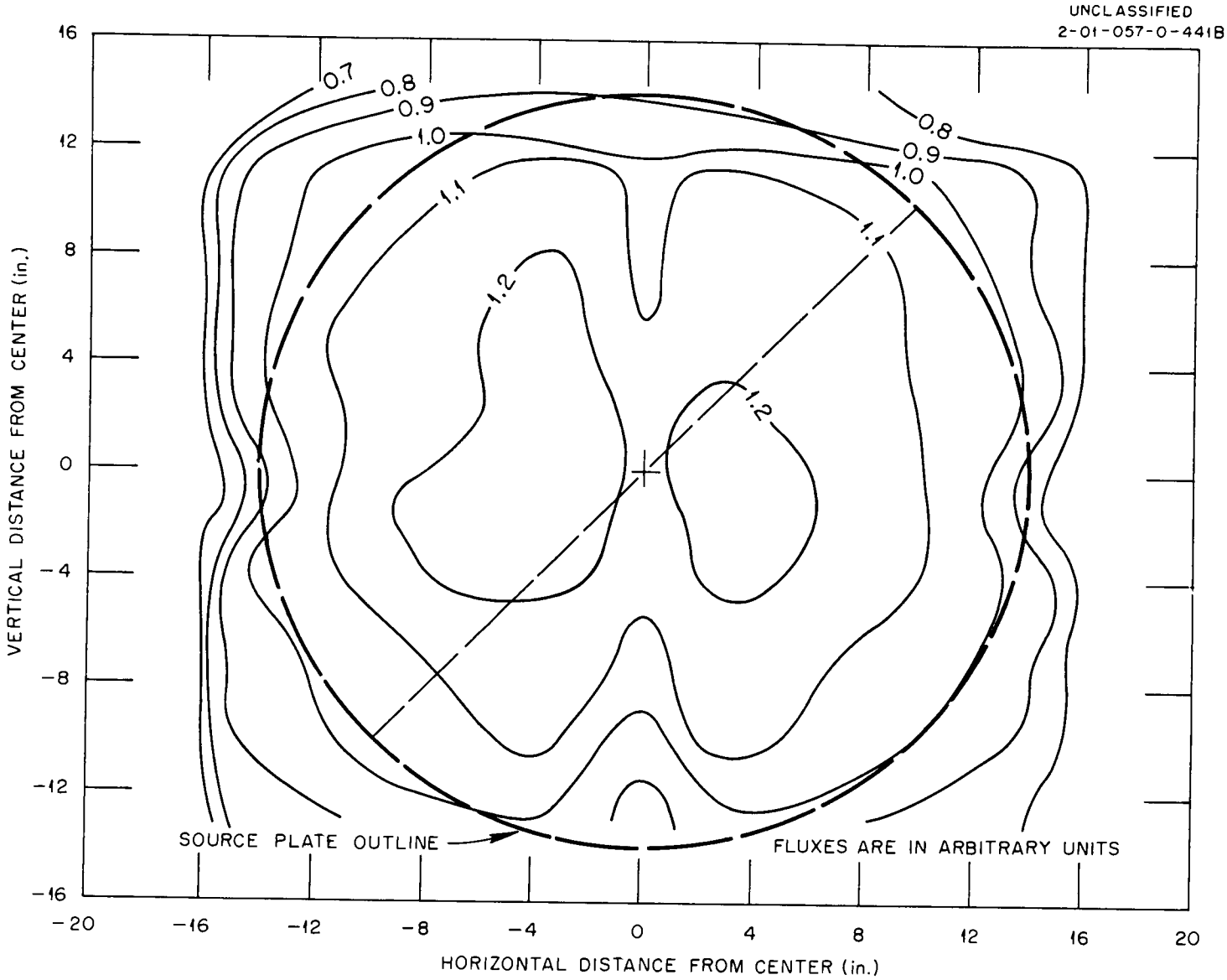

Fig. 6. Relative Core Hole Isoflux Plot (Looking Into the Graphite Reactor).

G = inverse square geometry correction for difference in locations of gold wires and source plate,

N = factor to normalize to the standard incident thermal-neutron flux,

L = factor to normalize to the configuration finally installed between the source plate and the reactor (see discussion below),

B = correction for leakage of boral shutter,

S = source plate area.

The numerical value of each of these is given in Table 1.

The normalizing factor L used in Eq. 1 was introduced to account for the 1-in.-thick lead slab which was installed between the SP-2 and the reactor after the experimental determination of $\emptyset$ was made. The value of L was based on the relative thermal-neutron flux levels in the LTSF with and without the lead in position (see p. 24).

Table 1. Numerical Values of Terms Used in Eq. 1

Term	Numerical Value	Estimated Error
$\emptyset$	1.35×10^{8} neutrons$\cdot$cm$^{-2}\cdot$sec^{-1}	4.6% (a)
f	0.575	5.0% (b)
v	0.826	2.0%
G	0.919	3.0%
N	1.00	5.0%
L	0.788	6.0%
B	0.971	0.5%
S	3980 cm^{2}	0.2%
P	1.79×10^{11} fissions/sec	11.0%

a. The quoted error in $\emptyset$ includes uncertainties in corrections for self absorption in the foils, reproducibility, etc., but does not include uncertainties generated by lack of knowledge of the energy and angular distribution of the incident neutrons.

b. The quoted error in f is supposed to cover uncertainties in f$\emptyset$ generated by lack of knowledge of incident energy and angular distribution.

The factor B was included to account for the fact that the boral shutter shown in Fig. 3 is not completely black to the Core Hole thermal neutrons. It is the practice at the LTSF to subtract readings taken with the shutter closed from readings taken with the shutter open in order to determine the background that is present. It has been established experimentally, however, that with the shutter closed the source plate is caused to fission at 2.9% of the open-shutter rate due to neutron leakage through the shutter. This means that 2.9% of the source plate strength is normally subtracted as background, and the fission rate that should be reported should be the fission rate in excess of that occurring when the shutter is closed.* (In the other two methods used to determine the source strength of the SP-2 this correction was unnecessary since the shutter-closed fission rate was subtracted out in the experiment.)

The strength of the source plate determined by this method is 1.79×10^{11} fissions/sec $\pm$ 11%. The error was based upon the root of the sum of the squares of the individual errors listed in Table I.

Method 2: Fission Rate Determination by Estimation of Neutron Production in the Source Plate

Since the number of neutrons emitted per thermal fission of U^{235} is known,[7] the fission rate in the source plate can be estimated on the basis of the rate of neutron production in the source plate. In this second method for determining the source strength of the SP-2, the rate of neutron production was estimated from thermal-neutron fluxes measured at the surface of the source plate assembly opposite from the reactor and throughout the Lid Tank proper. The steps of the method are described below.

It was assumed that each infinitesimal volume element of the uranium disk emits neutrons isotropically, and, since the disk is thin, it was further assumed that only a small number of these neutrons undergo collisions within the uranium. Therefore, one-half of the fission neutrons are emitted from either side of the uranium disk. The fission neutrons leaving the source plate in the direction of the Lid Tank have the following fate:

---

7. D. J. Hughes and J. A. Harvey, Neutron Cross Sections, BNL-325 (1955)

*See discussion of boral shutter on p. 7.

(1) Some are scattered or absorbed within the source plate assembly without ever reaching the Lid Tank.

(2) Some enter the Lid Tank but are scattered out again before they are thermalized.

(3) Some enter the Lid Tank and remain there long enough to become thermalized, after which they are (a) absorbed by the water in the Lid Tank or (b) diffused back into the source plate assembly and absorbed by the boral plate (see Fig. 3).

With each of these possibilities considered, the fission rate of the source plate can be estimated from the following equation:

$$P = 2\,\frac{n_1 + n_2}{\nu\, p_1 p_2} \tag{2}$$

where

n_1 = rate of neutron absorption in Lid Tank water (neutrons/sec),

n_2 = rate at which neutrons that re-enter the source plate assembly are absorbed in the boral (neutrons/sec),

ν = number of neutrons produced per fission[7]

= (2.45 ± 0.04) neutrons/fission,

p_1 = fraction of neutrons that leave the fission site in the uranium disk in the direction of the Lid Tank and escape the source plate assembly,

p_2 = fraction of neutrons that enter the LTSF water and remain there until thermalized.

The fraction p_1 depends upon the scattering and absorption cross sections as well as the dimensions of the materials composing the source plate assembly. By using fast-neutron total and absorption cross sections in place of gamma-ray cross sections in a reduction of Eq. A-2 of Appendix A, the absorption of neutrons in the source plate assembly is estimated to be almost 2%, so p_1 is equal to 0.98.

The fraction p_2 was determined by using a very simplified method for calculating fast-neutron albedoes. It was concluded that the fast neutrons scattered out of the Lid Tank are approximately compensated for by fast neutrons scattered into the Lid Tank from the surroundings, including the 1-in. lead slab. Therefore the fraction p_2 was taken to be unity.*

The value of n_1 was obtained from extensive X, Y, and Z thermal-neutron flux traverses in the Lid Tank (the Z axis coincides with the source plate axis). These measurements were made with a 1/2-in. fission chamber that was standardized against gold foil activations** which were interpreted by a procedure developed by Burrus that included corrections for flux depression and self shielding. The complete mapping of the Lid Tank took several weeks, many of the points being repeated on different days. The reproducibility of the measurements was generally within 15%.

In order to determine the value of n_1 from these traverse measurements it was assumed that the number of neutrons captured in an infinitesimal volume of the Lid Tank water was simply

$$dn_1 = \Sigma_a \phi_{th} dV \tag{3}$$

where Σ_a is the absorption cross section for thermal neutrons in water and ϕ_{th} is the observed thermal-neutron flux. The total number of thermal neutrons absorbed by the water was then obtained by integrating over the entire tank volume. A plot of the neutrons absorbed in the X,Y plane is given as a function of Z in Fig. 7. The integral of this curve gives a value of 13.4×10^{10} neutrons sec^{-1} for n_1.

---

* In the preliminary analysis of the source plate power reported in Paper I-H of ORNL-2115, Vol. I (classified), a value of $(n_1 + n_2)/p_2$ was obtained by defining an "effective" thermal-neutron flux that attempted to correct for the flux depression in the region of the source plate assembly. This approach was abandoned in favor of the present approach where p_2 is estimated from the albedo of fission neutrons entering the water and n_2 is obtained by estimating the thermal-neutron current into the boral sheet. This approach also includes the effect represented by p_1 which was not previously considered.

**This work was performed by W. R. Burrus and W. J. McCool.

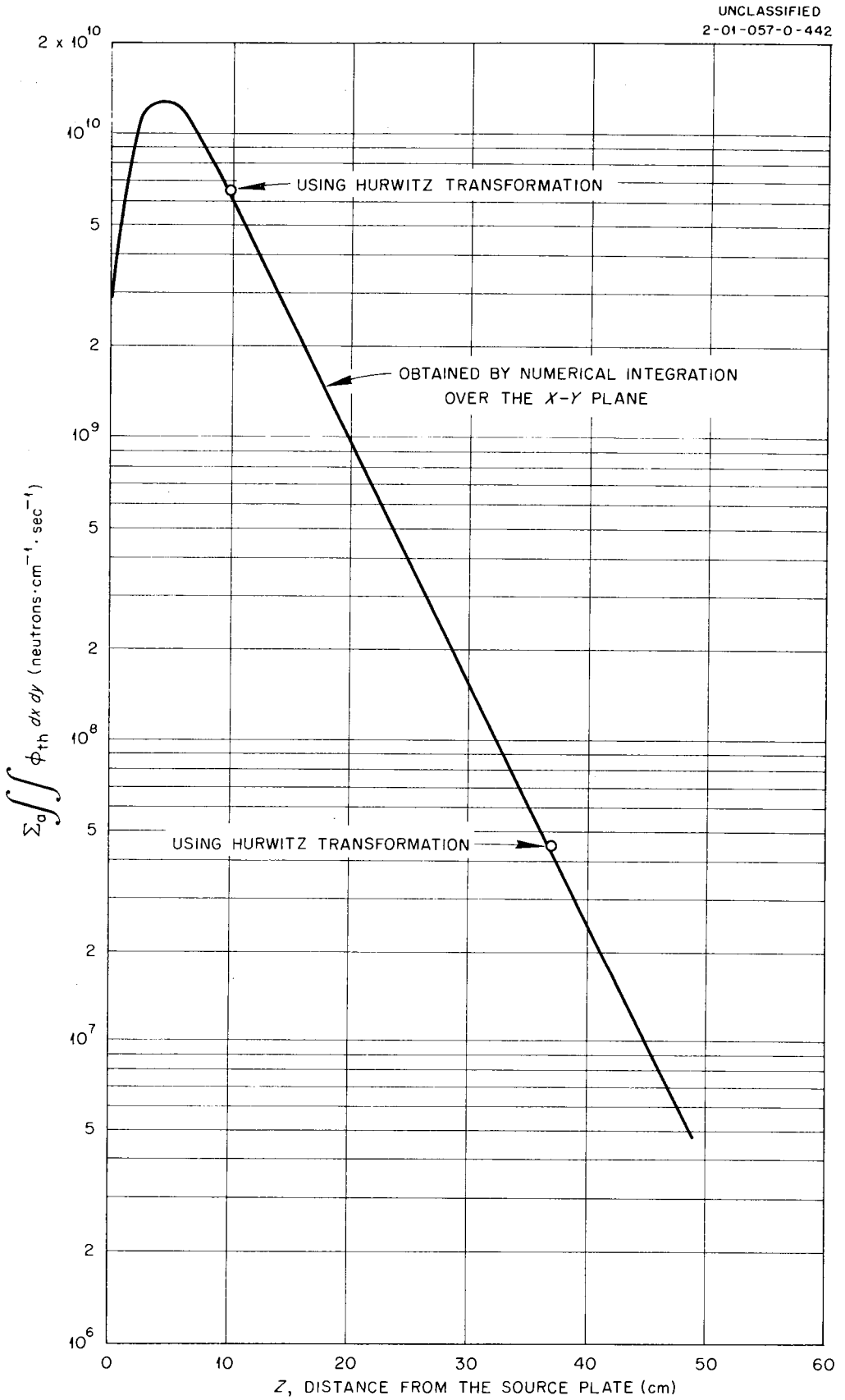

Fig. 7. Neutron Absorption Rate in Water in the X-Y Plane Per Unit Thickness as a Function of Z.

For purposes of comparison, a second nearly independent method was used for checking two points on the curve in Fig. 7. The Hurwitz correction[8] was used to obtain the thermal-neutron flux which would have been observed for an infinite disk source of the same specific strength as that of the SP-2, $\phi_{th}(Z,\text{inf})$. If I(Z) is the function plotted in Fig. 7, and S is the source plate area, then it can readily be shown that $I(Z) = S\phi_{th}(Z,\text{inf})$, the major assumption being the use of the Hurwitz transformation for a semi-infinite medium. As can be seen from Fig. 7, the results agreed within 5% with those obtained by the method discussed in the preceding paragraph.

The thermal-neutron current into the boral plate of the source plate assembly was calculated from the measured thermal-neutron flux at the surface of the source plate assembly by assuming a Fermi angular distribution[9] for the thermal neutrons. The Fermi distribution is

$$f(\psi) \sim \cos\psi + \sqrt{3}\cos^2\psi \tag{4}$$

where $f(\psi)$ is the angle-differential neutron current (neutrons$\cdot$cm$^{-2}\cdot$sec^{-1}) crossing one square centimeter of the interface and moving in the direction having an angle ψ to the normal. Although this distribution is an approximation for the angular distribution of thermal neutrons escaping from a block of paraffin into a void, its use for this case is justified on the basis that a void is essentially the same as a strong absorber (in this case, boral) and that the diffusion through water does not differ in principle from the diffusion through paraffin. The neutron current for a Fermi distribution related to the integral flux is

$$J = \phi/\sqrt{3} \tag{5}$$

8. S. Glasstone, Principles of Nuclear Reactor Engineering, D. Van Nostrand Company (1955).
9. E. Fermi, Revs. Mod. Phys. 9, No. 2, p. 132 (1937).

and the total flow of neutrons into the boral plate is obtained by integrating J over the area of the boral cover of the source plate:

$$n_2 = \frac{1}{\sqrt{3}} \int_A \phi_{th}(Z = 0)dA \tag{6}$$

where $\phi_{th}(Z = 0)$ is the thermal-neutron flux measured at the surface of the boral. The value for n_2 obtained by numerically evaluating this integral was 6.3×10^{10} neutrons/sec.

The values and their estimated errors for all the variables used in Eq. 2 are summarized in Table 2. In this case it was not necessary to include a normalization factor to account for the presence of the 1-in.-thick lead slab between the source plate and the reactor, as was done in Method I, since all the thermal-neutron measurements used in the calculation were obtained after the lead slab had been installed. The data were normalized to a constant source plate power as indicated by the Core Hole flux monitor.

Table 2. Numerical Values of Terms Used in Eq. 2

Term	Numerical Value	Estimated Error
n_1	13.4×10^{10} neutrons/sec	15%
n_2	6.3×10^{10} neutrons/sec	20%
ν	2.46 neutrons/fission	1.6%
p_1	0.98	1%
p_2	1.00	5%
P	1.64×10^{11} fissions/sec	13.5%

The strength of the source plate calculated by this method is 1.64×10^{11} fissions/sec $\pm$ 13.5%. As was done in Method I, the error was based upon the root of the sum of the squares of the individual errors.

Method 3: Fission Rate Determination by Estimation of Power Dissipation in the Source Plate*

At the time the SP-2 assembly was fabricated resistance gages were

*Much of the preliminary analysis of these data was performed by W. J. McCool.

cemented to the uranium disk at nine locations (see Fig. 2) so that the temperature of the source plate could be measured under various conditions. In addition, an electric heater plate was placed in immediate contact with the uranium disk so that it could be artifically heated with electricity. By comparing the temperature response of the source plate while it was undergoing fission with its response while it was being heated with a variety of known electrical powers, it was possible to determine the energy dissipation in the uranium during fission runs. Since the energy release per fission is known, the fission rate of the SP-2 could then be determined from the observed energy dissipation, thus providing a third method for determining the strength of the source plate.

The electric heater and resistance gages are described in Section I. The electric power was determined to within an accuracy of 0.9% by measuring the current flowing through the heater and the voltage drop across the heater. Gage resistances equivalent to local source-plate temperatures were measured with a Leeds and Northrup wheatstone bridge to within an accuracy of 0.1 ohm (almost $0.2^{\circ}F$)

Ten different electric power runs were made with input powers ranging from 3.7 to 16.4 watts. Five different fission power runs were made. Prior to each run, temperature response measurements were taken for approximately 1/2 hr to insure that the assembly was in thermal equilibrium. A single run required about 5 hr, during which time the source plate temperature was measured at 5-min intervals at each gage location. During the electric runs the input power was measured at 1-hr intervals.

Since for these runs the energy dissipation in the uranium disk was small, it was necessary to insulate the source plate assembly from its surroundings in order to obtain a measurable temperature rise. Several different schemes were tried, three of which are shown in Fig. 8. A 6-in. thickness of Styrofoam (an insulating material composed of Polystyrene foam) was placed in the LTSF adjacent to the source plate assembly in configuration a, while in configuration c the Styrofoam was placed on both sides of the assembly. In configuration b the styrofoam insulator was positioned on the outside of the assembly only and a 1-in.-thick slab was installed between the source plate assembly and the reactor.

UNCLASSIFIED
2-01-057-0-44

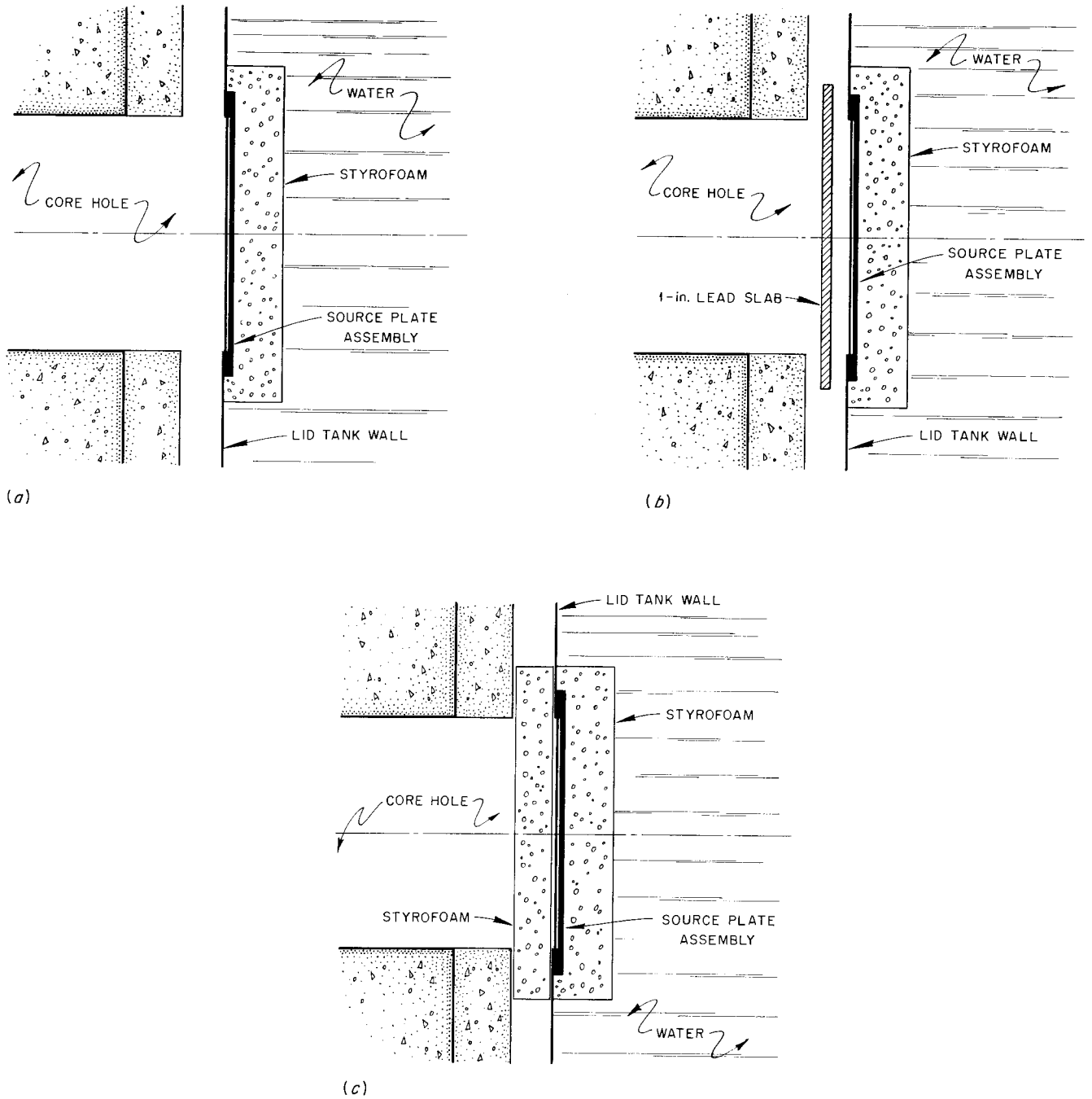

Fig. 8. Insulator Configurations Used in Temperature vs. Time Run in Energy Dissipation Experiment.

The lead in configuration b was used not as insulating material but because it had by this time been decided that a lead shield should be permanently installed as part of the SP-2 assembly to reduce the reactor gamma-ray background in the Lid Tank. Since the presence of any material between the source plate and the reactor during fission runs causes the thermal-neutron flux from the Core Hole to be attenuated and scattered before it reaches the source plate and hence affects the source plate power, it was necessary to normalize all the fission runs to a configuration which had the lead. Thus one fission run was made with configuration b and all of the other runs were normalized to it. The normalization was based upon the relative thermal-neutron flux levels in the Lid Tank for the three configurations.

Seven of the electric power runs were made with configuration a, which for these runs is essentially the same as configuration b, and three were made with configuration c. For reasons given below, the configuration c runs were not used to determine the final power result.

The temperature history of one resistance gage (No. 7, 1 in. east of the center) for five of the electric power runs and for one unnormalized fission run, all with configuration a, is shown in Fig. 9. Points were selected from each of the electric heating runs at 1/2-hr intervals and cross-plotted in Fig. 10 as curves of the temperature response as a function of the power input for several total heating times. A first estimate of the source plate power was then obtained by fitting temperature changes of the fission power run for the same heating times on the curves for the electric power runs. A line drawn through these points, shown as triangles in

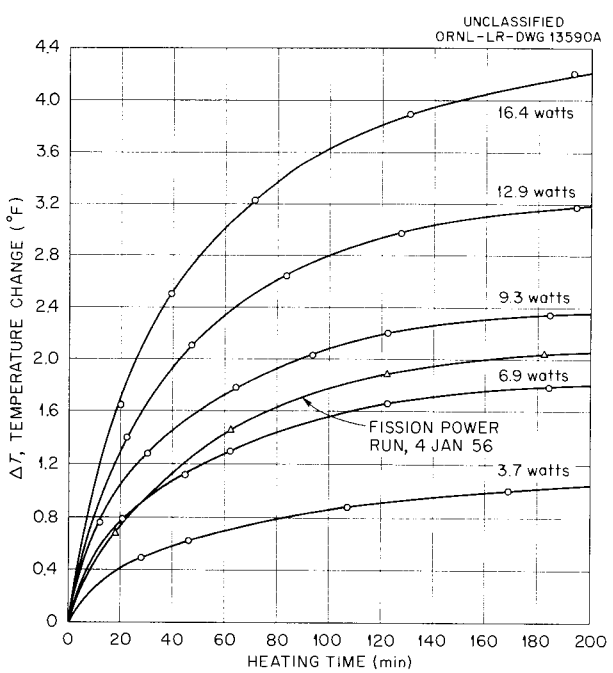

Fig. 9. Lid Tank Source Plate Power Calibration. Temperature response as a function of time for different power inputs (Resistance gage number 7, near center).

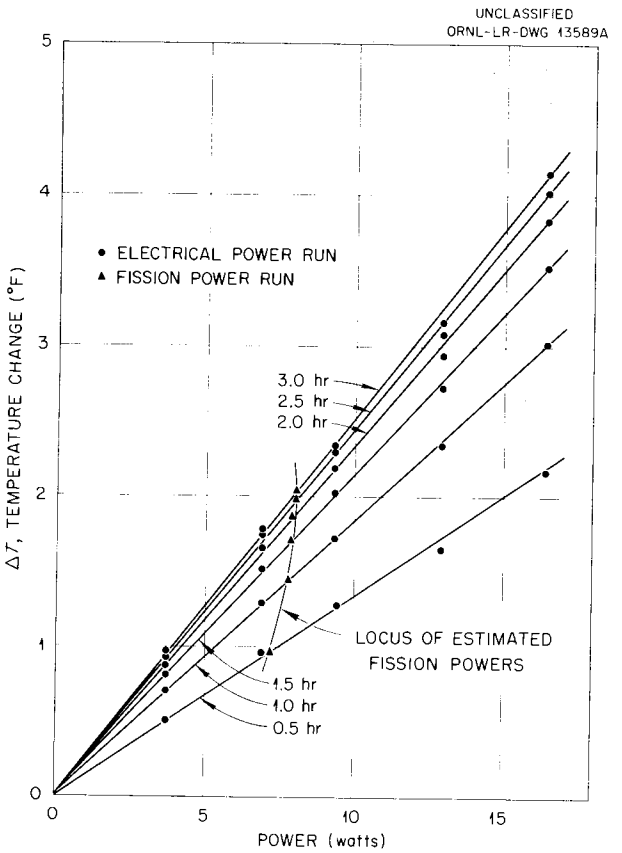

Fig. 10. Lid Tank Source Plate Power Calibration. Temperature Response as a Function of Power Input for Different Heating Times (Resistance Gage Number 7).

Fig. 10, indicates that the power estimated in this manner increases considerably with increasing total heating times. Similar plots were made for all fission runs and all resistance gages, and in each case it appeared that the estimated power varied in a systematic manner with the total heating time. (Possible reasons for this behavior are discussed in App. B.) It was concluded that the most accurate power estimate would be obtained by extrapolating the power to zero heating time since here the effect of variable heat-transfer coefficients is minimized. This was done with cross-plots of the estimated power as a function of the time of heating for each of the five fission runs. Typical plots are shown in Fig. 11. Power estimates based on the extrapolations are summarized in Table 3.

All extrapolations were made using power estimates calibrated on the basis of the seven electric heating runs which were obtained using insulator configuration a. For heating times greater than one hour, the three electric heating runs made using configuration c yielded a greater temperature response than did those using configuration a, but 1/2 hr after the heating began the results were indistinguishable. Since extrapolations to zero heating time were made, this evidence was considered adequate to justify the use of the configuration a calibrations for all data. Appendix B discusses why the extrapolated power values are independent of heat-transfer coefficients.

Table 3. Power Estimates Based on Five Fission Runs

Run No.	Date	Configuration (see Fig. 8)	Estimated Power ± 5% (watts)
1	12-28-55	a	6.59
2	12-30-55	a	6.81
3	1-4-56	a	6.64
4	12-20-55	b	4.41
5	1-6-56	c	5.33

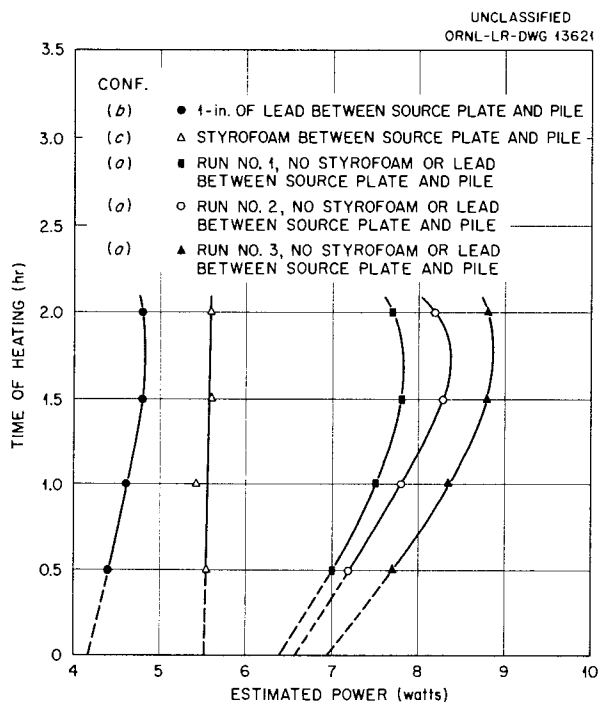

Fig. 11. Estimated Power as a Function of Time after Start of Heating.

The combination of the results given in Table 3 to obtain an average power estimate was accomplished by a weighting process in which the weight was determined by the inverse square of the errors. The procedure was as follows:

(1) All runs were assumed to have random errors of ±1% for a measurement error and ±5% for possible shifts in the ambient conditions.

(2) Runs 1, 2, and 3, all with configuration a, were averaged to yield 6.68 ± 0.213 watts.

(3) Run 5 was normalized to configuration a with a normalization factor of 1.21 ± 5% based upon the relative thermal-neutron fluxes in the LTSF for the two configurations. The normalized value was then combined with the average value for Runs 1, 2, and 3 to give a weighted average value of 6.68 ± 0.20 watts.

(4) Runs 1, 2, 3, and 5 were then normalized to configuration b with a normalization factor of 0.741 ± 6.2% based upon the relative thermal-neutron fluxes in the LTSF. The normalization error was considered to be systematic for Runs 1, 2, 3, and 5. The resulting power for these four runs was 4.95 ± 0.34 watts.

(5) The power obtained from Runs 1, 2, 3, and 5 was then averaged with the power obtained for Run 4. The final weighted average was 4.68 ± 0.24 watts.

The energy per fission absorbed by the source plate assembly was calculated to be 180 ± 3 Mev/fission (see App. A). Therefore, the fission rate in the source plate calculated by this method is 1.63×10^{11} fissions/sec ± 6%.

Summary of Methods 1, 2, and 3 in Terms of Power

The estimates of the source plate fission rate can be summarized as follows:

(1) Method 1, based on the thermal-neutron absorption in the source plate, gives a value of 1.79×10^{11} fissions/sec ± 11%.

(2) Method 2, based on the production of neutrons in the source plate, gives a value of 1.64×10^{11} fissions/sec ± 13.5%.

(3) Method 3, based on the energy dissipation in the source plate, gives a value of 1.63×10^{11} fissions/sec ± 6%.

A weighted average of these three values, where the weights are determined by the inverse square of the absolute error, yields 1.66×10^{11} fissions/sec ± 5%.

Usually it is more convenient to think of the source strength in terms of power in watts rather than in fissions per second. With an assumed energy dissipation of 200 Mev/fission, a number commonly used for calculating reactor core energy dissipation, the LTSF source plate produces neutrons at a rate equivalent to a reactor having a power of 5.22 watts ± 5%.* Since the source plate area is 3980 cm^2, the equivalent power per unit area is 1.31×10^{-3} watts/cm^2 ± 5%.

---

*Here and elsewhere in this report quoted errors are estimated standard deviations.

It should be remembered that the source strengths given above do not account for the attenuation of the radiations by the source plate assembly. Both the neutron and the gamma-ray powers of the SP-2 can be determined by applying the "effective leakage factors" described in App. C.

III. RE-EVALUATION OF THE POWER OF THE FIRST LTSF SOURCE PLATE (SP-1)[10]

The power of the first LTSF source plate, now identified as the SP-1, was never accurately known. It was originally quoted as 6 watts, a power based upon several measurements of the transient temperature response of the central fuel slugs that made up the source assembly. Later a neutron leakage factor of 0.6 was introduced in order to account for the neutron attenuation within the assembly. This resulted in a quoted effective power for neutrons of 3.6 watts.

The present power calibration of the SP-2 allows a re-evaluation of the estimated power of the SP-1 by a method in which the thermal-neutron fluxes and the gamma-ray dose rates along the z axis (the source plate axis) of the Lid Tank are compared for the two sources. Such comparisons are given in Figs. 12 and 13.

From the thermal-neutron data in Fig. 12 it can be seen that the flux for SP-1 is lower than the flux for SP-2 by a factor of 2.9 $\pm$ 10%. Since the power of SP-2 has been determined to be 5.22 watts and the neutron leakage factor to be 0.94 (see App. C), the "effective neutron power" of SP-1 was

$$P_n(\text{SP-1}) = \frac{5.22 \times 0.94}{2.9} = 1.7 \text{ watts} \pm 11\% \tag{7}$$

10. This information was previously presented by J. Smolen, ORNL-2081 op.cit., p. 164.

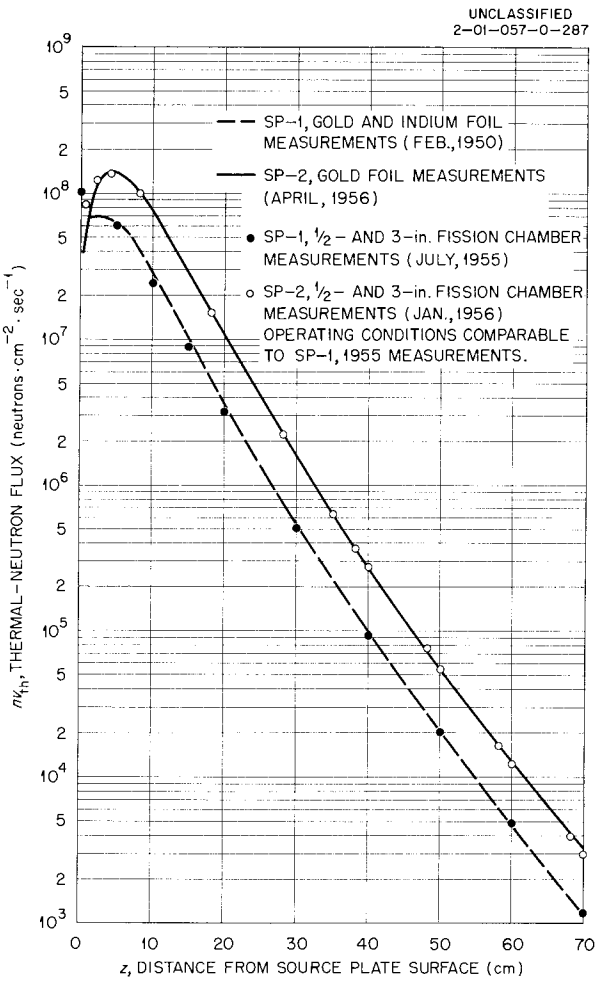

Fig. 12. A Comparison of the Thermal-Neutron Flux in the Water of the LTSF with Source Plates SP-1 and SP-2.

A comparison of the gamma-ray dose-rate measurements in Fig. 13 yields a ratio of approximately 4.0. This ratio is higher than the ratio for neutrons owing to the relatively higher gamma-ray absorption in the SP-1 assembly. The gamma-ray leakage factor for SP-2 is 0.88 (see App. C); therefore, the "effective primary gamma-ray power" of the SP-1 was

$$(8) \quad P_\gamma(\text{SP-1}) = \frac{5.22 \times 0.88}{4.0}$$

$$= 1.15 \text{ watts} \pm 20\%$$

The large error assigned to the gamma-ray power of SP-1 is necessary because the gamma-ray dose-rate curves shown in Fig. 13 include major contributions from secondary gamma rays produced by neutron captures in the water in the LTSF structure. The ratio of the secondary contributions for SP-1 and SP-2 would equal the ratio of the neutron flux rather than the ratio of the primary gamma-ray dose rate. Therefore, the ratio of 4.0 is not really the correct one, and the large error is assigned to account for

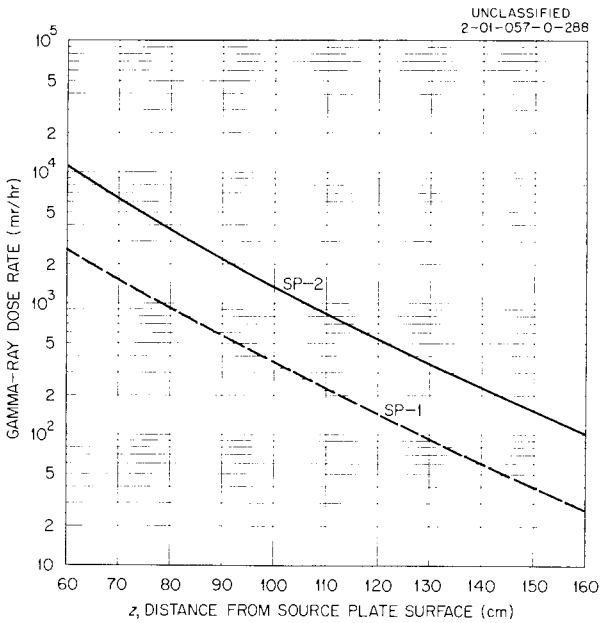

Fig. 13. Comparison of the Gamma-Ray Dose Rate in the Water of the LTSF with Source Plates SP-1 and SP-2.

this uncertainty. Great caution should be exercised in attempting to apply an "effective gamma-ray power" to the SP-1 data since secondary gamma rays usually constitute the greatest part of the total dose rate measured beyond shielding configurations.

App. A. FISSION ENERGY ABSORBED BY THE SP-2

(Referred to on pages 17 and 27 of text.)

The power dissipation per fission in the core of a nuclear reactor depends on the core construction, the composition of the fuel, and the geometry and composition of the reactor system surrounding the core. In reactors in which the fuel is circulated, the power dissipation also depends upon the rate of fuel circulation. Fortunately, the energy dissipation per fission can seldom vary more than $\pm 5\%$ from one reactor design to another, but the energy leakage from the thin source plate considered here is considerably more than that from a typical reactor. The precision desired from this work requires a separate estimate of energy escape from the region of the assembly in thermal contact with the uranium disk.

For the calculation of the energy dissipation in the source plate, only the region from the electric heater plate to the aluminum cover plate is considered since the resistance gages on the source plate would not be influenced by energy dissipated outside this region. The effect of the boral sheet under the cover plate was considered to be equivalent to that of the aluminum. A cross section of the configuration used in the calculation is shown in Fig. A-1 on p. 35.

The sources which are considered are (1) fission fragments with their kinetic energy and the gamma rays, beta particles, and neutrinos associated with their eventual nuclear decay, (2) prompt gamma rays, (3) fission neutrons, (4) "nonproductive" thermal-neutron captures, and (5) capture of thermal neutrons in the boral plate adjacent to the uranium disk.

All the energy resulting from fission fragments and beta particles can be considered to be deposited within the region specified above; therefore, the energy releases reported by Stein[11] for fission fragments and by King and Perkins[12] for beta particles are used directly. Conversely, all the neutrino energy is carried away from the source plate assembly.

---

11. W. E. Stein, Phys. Rev. 108, 94 (1957).
12. R. W. King and J. F. Perkins, Phys. Rev. 112, 966 (1958).

The effect of the gamma and neutron radiations is not so straightforward, however, and must be calculated for the region of interest.

In order to estimate the fraction of the gamma-ray energy absorbed, the following integral, based on first-collision energy absorption for an infinite source plate, was calculated:

$$\text{(A-1)} \qquad F = \frac{1}{2} \int_0^{\infty} n(E)dE \int_0^{t_U} P(t_3)dt_3 \left\{ \int_0^{t_U - t_3} \mu_{a_1} dz \int_z^{\infty} \frac{dR}{R} e^{-\mu_1 R} \right.$$

$$+ \int_{t_U - t_3}^{t_U - t_3 + t_2} \mu_{a_2} dz \int_z^{\infty} \frac{dR}{R} \exp - \left\{ (R/z) \left[\mu_1 t_1 + \mu_2 (z + t_3 - t_U) \right] \right\}$$

$$+ \int_0^{t_3} \mu_{a_3} dz \int_z^{\infty} \frac{dR}{R} e^{-\mu_3 R}$$

$$\left. + \int_{t_3}^{t_3 + t_4} \mu_{a_4} dz \int_z^{\infty} \frac{dR}{R} \exp - \left\{ (R/z) \left[\mu_3 t_3 + \mu_4 (z - t_3) \right] \right\} \right\}$$

where the regions are defined in Fig. A-1 on p. 35, and

F = gamma-ray energy absorbed in the source plate assembly (Mev/fission),

$n(E)$ = prompt fission plus decay gamma-ray energy spectrum ($\text{Mev} \cdot \text{fission}^{-1} \cdot \text{Mev}^{-1}$);

$P(t_3)$ = power distribution in the source (cm^{-1}) normalized so that

$$\int_0^{t_U} P(t_3)dt_3 = 1$$

μ_{a_i} = energy absorption linear attenuation coefficient for gamma rays in the ith region (cm^{-1}),

μ_i = total linear attenuation coefficient for gamma rays in the ith region (cm^{-1}), modified to include approximate buildup for some calculations,

t_i = thickness of the ith region (cm),

t_U = thickness of uranium (cm) = $t_1 + t_3$ (see sketch in Fig. A-1),

t_4 = thickness of aluminum on reactor side of source plate (cm),

t_2 = thickness of aluminum and boral on Lid Tank side of source plate (cm),

z = dummy distance coordinate normal to the source plate surface (cm),

R = distance between source point and point of energy absorption.

The bracketed quantity was solved analytically* for the configuration shown in Fig. A-1 and is equal to

$$\text{(A-2)} \qquad f(t_3,E) = \left[\frac{\mu_{a_1}}{\mu_1} + \left(\frac{\mu_{a_2}}{\mu_2} - \frac{\mu_{a_1}}{\mu_1}\right)\left(e^{-\mu_1 t_1} - \mu_1 t_1 E_1(\mu_1 t_1)\right) - \frac{\mu_{a_2}}{\mu_2}\left(e^{-\mu_1 t_1 - \mu_2 t_2} - (\mu_1 t_1 + \mu_2 t_2)E_1(\mu_1 t_1 + \mu_2 t_2)\right)\right]$$
$$+ \left[\frac{\mu_{a_3}}{\mu_3} + \left(\frac{\mu_{a_4}}{\mu_4} - \frac{\mu_{a_3}}{\mu_3}\right)\left(e^{-\mu_3 t_3} - \mu_3 t_3 E_1(\mu_3 t_3)\right) - \frac{\mu_{a_4}}{\mu_4}\left(e^{-\mu_3 t_3 - \mu_4 t_4} - (\mu_3 t_3 + \mu_4 t_4)E_1(\mu_3 t_3 + \mu_4 t_4)\right)\right]$$

where

$\frac{1}{2}f(t_3,E)$ = fraction of gamma radiation of initial energy E absorbed within the source plate assembly with an infinite plane source located so that t_1 and t_3 are the thickness of uranium on either side.

*By R. W. Peelle.

$$E_1(x) = \text{exponential integral} = \int_x^{\infty} e^{-q} dq/q.$$

Equation A-1 can now be written as

$$F = \frac{1}{2} \int_0^{\infty} n(E)dE \int_0^{t_U} P(t_3)f(t_3,E)dt_3 \tag{A-3}$$

This integral was evaluated by graphical integration using the sum of the prompt gamma-ray spectrum given by Gamble[13] and the fission-product gamma-ray spectrum given by Peelle[14] for n(E) as shown in Fig. A-1. The result of the integration with respect to t_3 is shown in Fig. A-2 (curve identified as "best estimate"). This was obtained by applying exponential buildup factors, equivalent to using modified values for μ_i. Upper and lower limits of energy absorption are also shown in Fig. A-2. For the calculation of the upper limit, the total linear attenuation coefficient was also used for the absorption coefficient, which is equivalent to saying that every interaction results in complete absorption. The lower limit was obtained by using the proper values for μ_{a_i} and μ_i without considering buildup. Integrating the "best estimate" from Fig. A-2 with respect to E gives 3.3 Mev/fission for the energy dissipation in the source plate assembly by prompt and decay gamma rays. This is approximately 27% of the total energy of the gamma rays. Figure A-1 also shows the photon energy dependence of the absorbed energy.

The kinetic energy of the fission neutrons contributes about 5 Mev/fission to the energy deposition in a nuclear reactor, and the neutron binding energy released as capture gamma rays from neutron capture reactions amounts to as

---

13. R. L. Gamble, Prompt Fission Gamma Rays from Uranium-235, Thesis, Univ. of Texas (1955).
14. R. W. Peelle, W. Zobel, and T. A. Love, Appl. Nuclear Phys. Div. Prog. Rep. Sept. 10, 1956, ORNL-2081, p. 91.

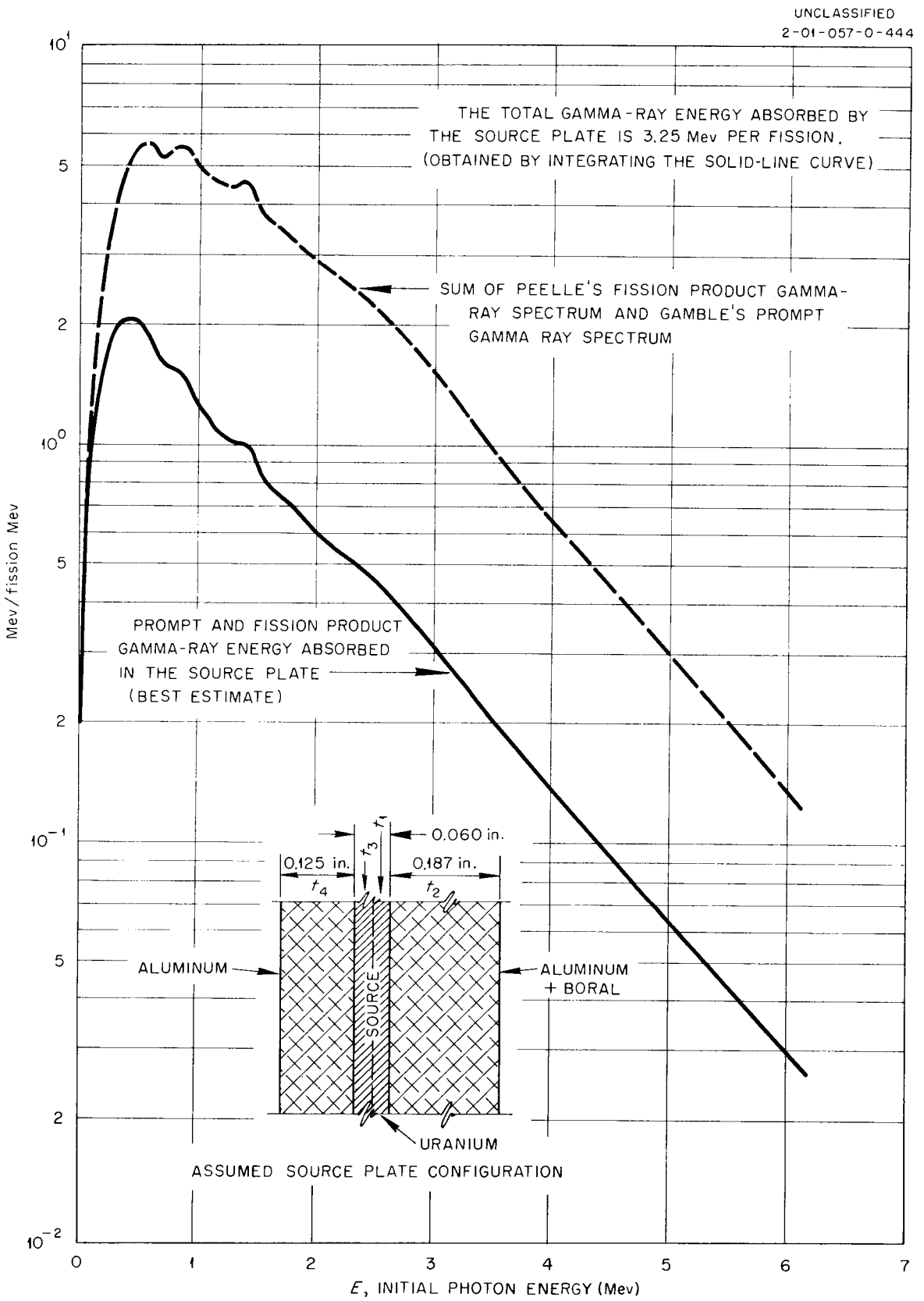

Fig. A-1. Gamma-Ray Energy Absorbed in the LTSF Source Plate (SP-2) as a Function of the Initial Photon Energy (Both Prompt and Fission Product Gammas).

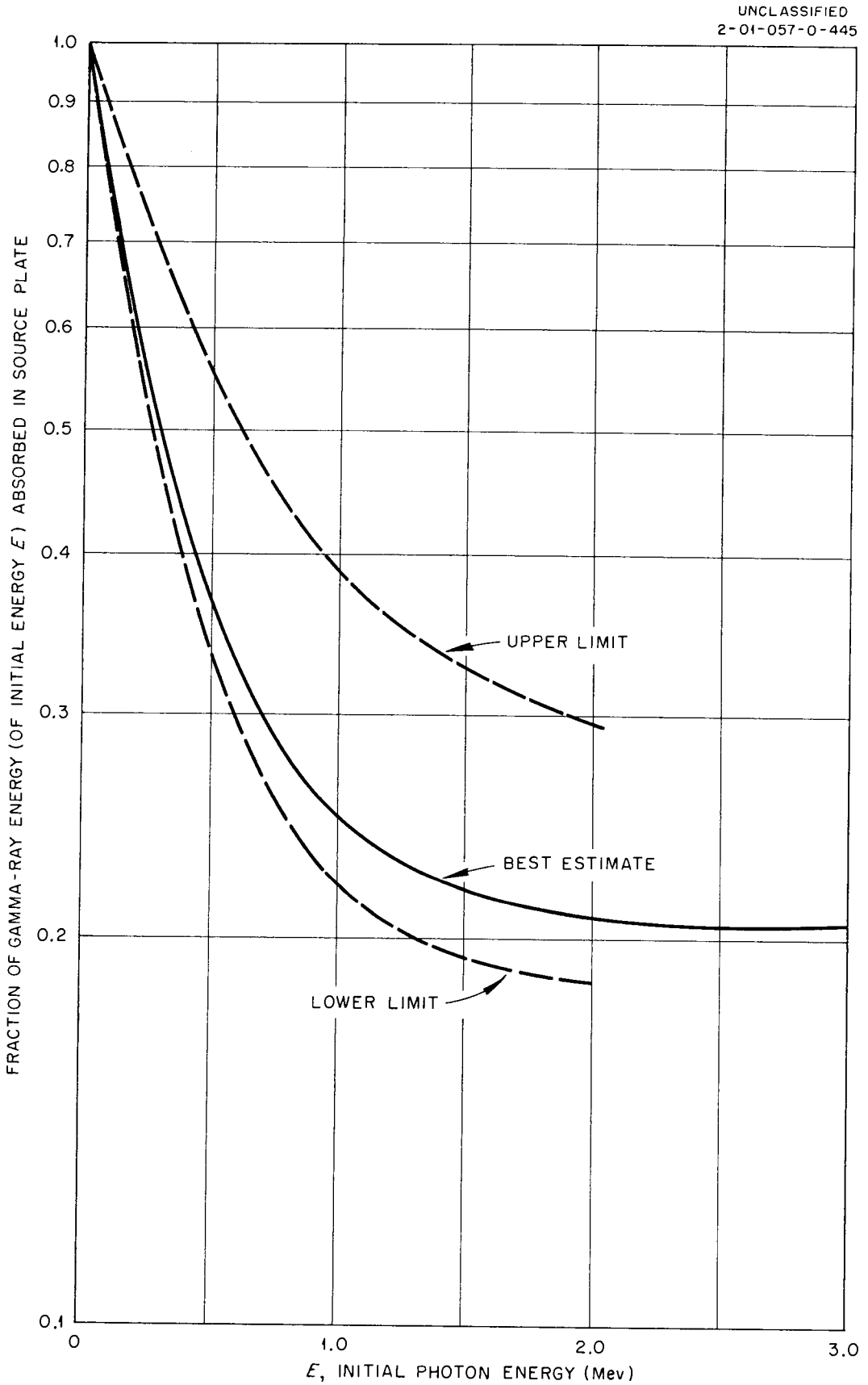

Fig. A-2. Fraction of Gamma-Ray Energy Absorbed in the LTSF Source Plate (SP-2) as a Function of Initial Photon Energy.

much as 10 Mev/fission, depending upon the reactor construction. In the case of the source assembly, no appreciable contribution is present from these sources because of the thinness of the plate. Absorption of neutron-capture gamma rays will amount to less than 0.3 Mev/fission because this process depends upon the return to the source assembly of gamma rays from thermal-neutron captures in the water and structure of the Lid Tank. Energy dissipation from fast neutrons can be considerably overestimated by replacing the gamma-ray cross sections of Eq. A-2 with typical fast-neutron total and nonelastic cross sections for the materials of the assembly. This results in an estimated absorption of only 0.1 Mev/fission.

"Nonproductive" capture of thermal neutrons from the reactor in the U^{238} and U^{235} of the source plate assembly also results in the deposition of energy. From the composition of the source plate and the known thermal-neutron cross sections for uranium, it can be shown that only 83% of the thermal neutron captures result in fission. Therefore, 17% of the captures are nonproductive insofar as the fission process is concerned. But these captures result in the emission of gamma rays. If a gamma-ray energy release of 5 Mev per nonproductive capture is assumed, the energy release is 1 Mev/fission. Since, as determined above, approximately 30% of these are absorbed in the source plate assembly, the energy dissipation attributable to nonproductive captures is 0.3 Mev/fission.

Thermal neutrons are absorbed in the boral adjacent to the source plate from sources on both sides of the plate. Under standard conditions, about 1.5×10^{11} neutrons/sec $\pm$ 15% from the reactor penetrate the uranium plate and are absorbed,* and 0.63×10^{11} neutrons/sec from the Lid Tank diffuse to the boral and are captured (see n_2 in Table 2). Each of these neutrons, about 1.4 per fission, releases about 2.7 Mev in the $B^{10}(n,\alpha)Li^7$ reaction, yielding a correction of 3.8 Mev/fission.

---

*Estimated from $\frac{P}{v} \cdot \frac{1-f}{f}$, where the symbols are defined in Method 1 of Section II.

The various sources of energy deposition are summarized in Table A-1. They result in an estimated energy absorption in the source plate of (180 ± 3) Mev/fission.

Table A-1. Energy Dissipation in the SP-2*

Energy Source	Energy Release (Mev/fission)	Fraction Deposited in Source Plate	Source Plate Energy Dissipation (Mev/fission)	Reference
Fission fragments	165 ± 2	1.00	165 ± 2	a
Beta particles	8 ± 1	1.00	8 ± 1	b
Prompt and fission-product gamma rays	12.1 ± 2	0.27	3.3 ± 0.6	c,d
Nonproductive captures of incident neutrons	1.0	0.30	0.3 ± 1	
Capture of thermal neutrons in boral	3.8 ± 0.8	1.0	3.8 ± 0.8	

* This table has been brought up to date with 1959 values that were not available in 1956 when this report was written.

a. W. E. Stein, Phys. Rev. 108, 94 (1957).

b. R. W. King and J. F. Perkins, Phys. Rev. 112, 966 (1958). (Error estimate and best value used were not given by these authors.)

c. R. L. Gamble, Prompt Fission Gamma Rays from Uranium-235, Thesis, University of Texas (1955).

d. R. W. Peelle, W. Zobel, and T. A. Love, Appl. Nuclear Phys. Div. Prog. Rep. Sept. 10, 1956, ORNL-2081, p. 91.

APP. B. ESTIMATED POWER OF SP-2 VERSUS HEATING TIME

(Referred to on page 25 of text)

In Section III it was pointed out that the estimated power derived from the temperature rise in the source plate appeared to vary systematically with the time of heating.* In this appendix possible reasons for this behavior are considered.

If the source plate response were the same for both electric and fission heating, the shapes of the curves in Fig. 9 would be similar, the estimated fission power points in Fig. 10 would lie on a vertical line, and the estimated source plate power would be independent of the period of heating. Since Fig. 9 demonstrates that such is not the case, differing thermal behavior of the source plate under the two conditions of heating is indicated. Possible reasons for this variation in behavior include differences in the locations of the heat sources, differences in the power distributions, and differences in the heat loss characteristics of the two heating systems.

The electric heat source consists of a spiral-wound wire adjacent to the outside face of the source plate, while the fission heat sources are scattered throughout the source plate. This difference in location will result in a difference in temperature distribution within the source plate assembly. In order to assess the order of magnitude of this difference, an estimate was made of the difference in temperature between the surface of the aluminum heater plate and the center of the source plate. For this calculation it was assumed that the heat production of the electric heater is 5 watts and that this amount of heat leaves the source plate along lines normal to the assembly with one-half of the energy being conducted in either direction. Using a thermal conductivity of 15.5 $Btu \cdot ft \cdot ft^{-2} hr^{-1} \cdot {}^{o}F^{-1}$ for the uranium and considering the steady state condition, since this gives the maximum temperature difference, gives an estimated temperature difference of $0.003^{o}F$. Since the temperature rise in the source plate after a 1/2-hr heating period is $\sim 0.8^{o}F$, and since no power estimates were based

*A small effect of this nature, inadequate to explain the observations, can be expected on the basis of the time dependence of the heating from fission-product gamma rays.

on heating times less than 1/2 hr, differences due to the location of heat source appear negligible and can be ignored.

The 1/2-in. spacing of the spiral of the electric heating wire causes nonuniformities in the electric power distribution. This effect may be considered by estimating the maximum temperature difference between the wire and a point on the aluminum heater plate halfway between two adjacent turns. This value was calculated as $\sim 0.001^{\circ}F$. Since this is negligible, the power distribution from electric heating may be assumed uniform.

The uniformity of the fission power production within the source plate should be directly dependent upon the uniformity of the thermal-neutron flux producing the fissions. Figure 6 shows the flux distribution for the Core Hole, indicating a variation of $\sim 10\%$ from the mean, with low points at the center and sides. Comparison of gage readings for the two conditions of heating showed no correlation between the estimated powers and the incident flux; in fact, gages located in the outer regions where the lowest fluxes were observed gave the highest estimates of power. However, since it was felt that these readings were unreliable because of low-temperature changes and poor thermal contact with consequent high thermal resistance, they were ignored in the analysis. Poor thermal contact at the edge is expected because the assembly is held together with hydrostatic pressure, and the edge of the plate is protected from this force by an aluminum shoulder.

The differences between electric heating and fission heating of the source plate are therefore most probably attributable to the heat loss characteristics of the two systems caused by the differences in the geometries for the electric and fission heating runs. The electric heating runs were made with the boral shutter of the Core Hole in the closed position, while, of necessity, the fission power runs required the shutter to be open. Convective heat losses from the Core Hole side of the source plate in the case of electric heating were restricted to the small volume of air between the source plate and the boral shutter. Opening the shutter for the fission runs changed the configuration by exposing the source plate to the end plate of the Core Hole, thus changing the heat transfer coefficients and ambient conditions.

The exact effect of this change is difficult to calculate; nevertheless, simple heat conduction systems can be considered in an attempt to understand the observed behavior. Each system can be described as an infinite slab insulated on one side, with convective heat loss on the other side and with internal heat generation. The thermal conductivities of the slabs are assumed to be infinite so that the temperature is constant across the slabs. Starting at zero time, heat is generated within the slabs at a constant rate, and the temperature increases until equilibrium is reached between the heat generation and the heat loss to the uninsulated side of the slabs. The systems are taken to be identical except that the boundary conditions differ in the values of the time-independent heat transfer coefficient and the ambient temperature, where the ambient temperature is the difference between the temperature of the surroundings and that of the plate at the start of the run. The two cases that we are considering refer to the conditions of electric heating and fission heating of the source plate, and the differences in heat-transfer coefficients and ambient conditions result from the opening and closing of the boral shutter and any failure in the procedure of having the source plate in equilibrium with all its surroundings at the time t = 0. They are also applicable to the differences between insulator configurations a, b, and c (see Fig. 8). The solution to the heat conduction equation giving the temperature as a function of time for one system is:

$$T_1 = \frac{(P_1 + h_1 T_{1a})}{h_1}\left(1 - e^{-\frac{h_1 t_1}{c}}\right) \tag{B-1}$$

where

t_1 = time after start of heating (sec),

c = heat capacity of system (Btu/^{o}F) (same for both cases),

h_1 = heat convection coefficient (Btu.^{o}F^{-1}.sec^{-1}),

P_1 = constant power dissipation (Btu/sec),

T_1 = temperature (^{o}F) at time t_1 where T_1 = 0 when t_1 = 0.

T_{1a} = ambient temperature (^{o}F), measured from source plate temperature at t_1 = 0.

(The other system will be designated by the subscript "2.") If two experiments were compared, one with fission power and the other with electric power, for which $T_1 = T_2$ when $t_1 = t_2 = t$, then the ratio of the powers for the two systems is given by:

$$\text{(B-2)} \qquad \frac{P_2 + h_2 T_{2a}}{P_1 + h_1 T_{1a}} = \frac{h_2}{h_1} \left[\frac{e^{-h_1 t/c} - 1}{e^{-h_2 t/c} - 1} \right]$$

If it were possible to specify the constants in this equation and if the assumptions corresponded more precisely to the real situation, the known power of the electrically heated system could be corrected to obtain the power of the fission-heated system for any time t after the start of the run. Although this is impossible, the equation may be used to provide an indication of the effects of nonequilibrium ambient conditions and differences in the heat-transfer conditions between the two runs.

Equation B-2 shows that the power ratio between cases which give the same temperature rise at time t is a function of the time, the amount of nonequilibrium temperature difference, and the heat-transfer coefficients. Even if it is assumed that $T_{2a} = T_{1a} = 0$, the powers are still unequal except at small times $\left[(ht/c) \ll 1\right]$ when Eq. B-2 becomes

$$\text{(B-3)} \qquad \frac{P_2 + h_2 T_{2a}}{P_1 + h_1 T_{1a}} = \frac{\left(1 - \frac{h_1 t}{2c} + \ldots\right)}{\left(1 - \frac{h_2 t}{2c} + \ldots\right)} \simeq 1$$

Thus if equilibrium has been achieved between the plate and its surroundings ($T_{1a} = T_{2a} = 0$), the power ratio approaches unity (linearly) at zero time. This is the justification for the extrapolation discussed in Method 3. The result is reasonable, since heat-transfer coefficients cannot be important until a temperature difference has been accomplished.

If ambient equilibrium has not been achieved or if the ambient temperature does not remain constant during a given run, there is no good way to relate P_1

and P_2 without knowing at least the values h_i. The difference observed between the various power estimates in Fig. 11 could be explained on such a basis.

App. C. DETERMINATION OF SOURCE PLATE LEAKAGE FACTORS

(Referred to on page 28 of text.)

Before the power of the SP-2 can be used in shielding calculations, the "effective leakage factors" for both neutrons and gamma rays must be determined. Effective leakage factors are derived to correct the source plate power for the effect of the absorption in the source plate assembly when radiation measurements are made beyond shield configurations.

In order to determine the primary gamma-ray leakage factor it was assumed that the dose rate measured at the outer surface of a typical shield configuration is largely from photons that had initial energies of about 3 Mev and were emitted along lines normal to the source plate surface. Buildup in the source plate assembly was neglected since the scattered component has a low probability of reaching the shield surface. Using the known total cross sections for 3-Mev photons in uranium and aluminum and the known geometry of the source plate assembly gives an effective leakage factor for primary gamma rays of 0.88. This factor is not valid for the usually more important secondary gamma rays, for which the production rate depends on neutron leakage from the plate.

The attenuation of fission neutrons by the source plate assembly was calculated using effective removal cross sections. This attenuation was based upon penetration normal to the source plate surface and is claimed valid only if > 50 g/cm^2 of hydrogenous material is interposed between the detector and the source. The calculated attenuation was 6%, resulting in an effective leakage factor of 0.94 for neutrons. Most of the attenuated (6%) fraction of the neutrons enter the tank and are captured relatively close to the source so the use of this factor should be avoided in the calculation of secondary gamma rays.

Where these "effective leakage factors" apply, they may be multiplied by the measured SP-2 strength to give the power of a truly "thin" disc which would yield the same result in the experiment of interest.

App. D. LIST OF FIGURES

Fig. No.	Title	Page No.
1	Sectional View of the First LTSF Source and Shutter (SP-1)	2
2	Exploded View of the Second LTSF Source Plate Assembly (SP-2)	4
3	Sectional View of the Second LTSF Source Plate (SP-2) Showing Its Position Relative to the Boral Shutter and the ORNL Graphite Reactor	5
4a	Mockup for Thermal Utilization Experiment	10
4b	Gold Wire Mockup for Flux Determination	10
5	Vertical Cross Section of the ORNL Graphite Reactor Core Hole Showing the Position of the Gold Foils and Wires in the Thermal Utilization Experiment (Lid Tank not shown)	11
6	Relative Core Hole Isoflux Plot (Looking into the Graphite Reactor)	14
7	Neutron Absorption Rate in Water in the X-Y Plane Per Unit Thickness as a Function of Z	19
8	Insulator Configurations Used in Temperature vs. Time Run in Energy Dissipation Experiment	23
9	Lid Tank Source Plate Power Calibration. Temperature Response as a Function of Time for Different Power Inputs (Resistance Gage Number 7, Near Center)	24
10	Lid Tank Source Plate Power Calibration. Temperature Response as a Function of Power Input for Different Heating Times (Resistance Gage Number 7)	25
11	Estimated Power as a Function of Time after Start of Heating	26
12	A Comparison of the Thermal-Neutron Flux in the Water of the LTSF with Source Plates SP-1 and SP-2	29
13	Comparison of the Gamma-Ray Dose Rate in the Water of the LTSF with Source Plates SP-1 and SP-2	30

Fig. No.	Title	Page No.
A-1	Gamma-Ray Energy Absorbed in the LTSF Source Plate (SP-2) as a Function of the Initial Photon Energy (Both Prompt and Fission Product Gammas)	35
A-2	Fraction of Gamma-Ray Energy Absorbed in the LTSF Source Plate (SP-2) as a Function of Initial Photon Energy	36

ORNL-2350
Physics and Mathematics
TID-4500 (14th ed.)

INTERNAL DISTRIBUTION

1. C. E. Center
2. Biology Library
3. Health Physics Library
4-6. Central Research Library
7. Reactor Experimental Engineering Library
8-43. Laboratory Records Department
44. Laboratory Records, ORNL R.C.
45. A. M. Weinberg
46. L. B. Emlet (K-25)
47. J. P. Murray (Y-12)
48. J. A. Swartout
49. E. H. Taylor
50. E. D. Shipley
51. A. H. Snell
52. W. H. Jordan
53. G. E. Boyd
54. E. P. Blizard
55. R. A. Charpie
56. M. L. Nelson
57. S. C. Lind
58. F. L. Culler
59. A. Hollaender
60. J. H. Frye, Jr.
61. M. T. Kelley
62. R. S. Livingston
63. K. Z. Morgan
64. L. S. Abbott
65. A. S. Householder
66. C. P. Keim
67. C. S. Harrill
68. C. E. Winters
69. D. S. Billington
70. H. E. Seagren
71. D. Phillips
72. A. J. Miller
73. R. R. Dickison
74. P. M. Reyling
75. G. C. Williams
76. J. L. Fowler
77. R. B. Briggs
78. L. Jung
79. F. L. Keller
80. F. C. Maienschein
81. J. M. Miller
82. R. B. Murray
83. R. W. Peelle
84. S. K. Penny
85. C. A. Preskitt
86. E. G. Silver
87. A. Simon
88. M. J. Skinner
89. D. K. Trubey
90-91. W. Zobel
92. C. E. Clifford
93. C. D. Zerby
94. A. D. Callihan
95. L. B. Holland
96. R. R. Coveyou
97-99. ORNL - Y-12 Technical Library, Document Reference Section

ORNL-2350
Physics and Mathematics
TID-4500 (14th ed. Rev.)

EXTERNAL DISTRIBUTION

100. Nuclear Development Corporation of America (Attn: H. Goldstein)
101-108. Convair, San Diego (Attn: C. E. Chapman, Dr. Donaldson, and 5 copies to D. R. Otis)
109. Curtiss-Wright Corp., Research Division, Quehanna, Pa. (Attn: K. L. Rooney)
110-116. General Electric, Cincinnati (Attn: F. A. Aschenbrenner, J. MacDonald, W. E. Edwards, J. Carver, R. H. Clark, L. S. Burns, and J. Haffner)
117-118. General Electric, Idaho (Attn: J. Van Hoomissen and E. Finauer)
119. Jet Propulsion Laboratory, Pasadena, Calif. (Attn: R. V. Meghreblian)
120. National Advisory Committee for Aeronautics, Cleveland, Ohio Attn: I. M. Karp)
121-122. Pratt and Whitney Aircraft (Attn: W. Kennedy and H. C. Woodsum)
123. Technical Research Group (Attn: R. Aronson)
124-125. The Martin Company (Attn: C. R. Fink and J. Weddell)
126-128. Wright Air Development Center (Attn: T. K. Krueger, L. A. Bowman, and J. R. Bohannon)
129. Wright Air Development Center at Brookhaven National Laboratory (Attn: R. D. Schamberger)
130. Battelle Memorial Institute (Attn: H. Epstein)
131-745. Given distribution as shown in TID-4500 (14th ed. Rev.) under Physics and Mathematics Category (75 copies - OTS)
746. Division of Research and Development, AEC, ORO